AD-A031 942 WISCONSIN UNIV MADISON MATHEMATICS RESEARCH CENTER F/G 20/12
MAGNETIC FLUX ANNIHILATION IN A LARGE JOSEPHSON JUNCTION.(U)
JUL 76 A C SCOTT DAAG29-75-C-0024
UNCLASSIFIED MRC-TSR-1649 NL

1 OF 1
AD A031942

END
DATE FILMED
1 -77

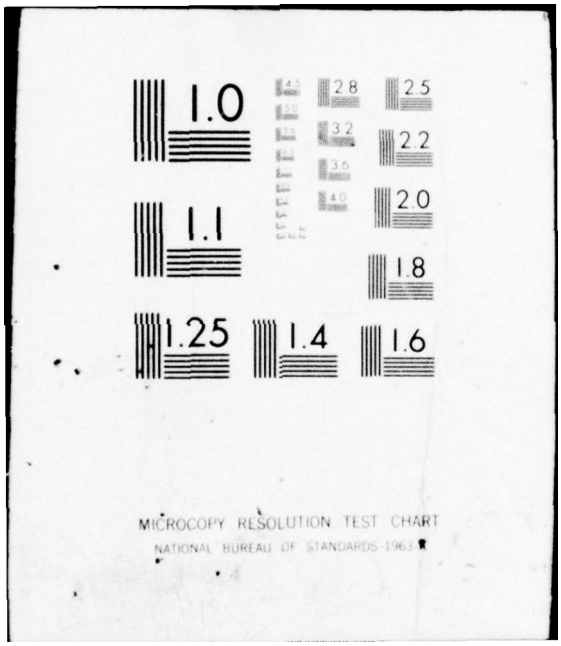
1.0
1.1
1.25
1.4
1.6
2.8
3.2
3.6
4.0
2.5
2.2
2.0
1.8
MICROCOPY RESOLUTION TEST CHART
NATIONAL BUREAU OF STANDARDS-1963-A

(11) FG

(9) MRC Technical Summary Report # 1649

(6) MAGNETIC FLUX ANNIHILATION IN A LARGE JOSEPHSON JUNCTION

(10) Alwyn C. Scott

(14) MRC-TSR-1649

Mathematics Research Center
University of Wisconsin—Madison
610 Walnut Street
Madison, Wisconsin 53706

(11) July 1976

(12) 65 p.

(Received April 2, 1976)

(15) DAAG29-75-C-0024
NSF-ENG-75-08492

Approved for public release
Distribution unlimited

Sponsored by

U. S. Army Research Office
P. O. Box 12211
Research Triangle Park
North Carolina 27709

and

National Science Foundation
Washington, D.C. 20550

221 200
bpy

UNIVERSITY OF WISCONSIN - MADISON
MATHEMATICS RESEARCH CENTER

MAGNETIC FLUX ANNIHILATION IN A LARGE JOSEPHSON JUNCTION

Alwyn C. Scott

Technical Summary Report #1649
July 1976

ABSTRACT

Recent developments in the theory of the sine-Gordon equation are used to analyze the appearance of a "displaced linear branch" in the volt-ampere characteristic of a large Josephson junction. Internally the junction is divided into a flux annihilation domain near the center and flux flow domains near the edges. The displaced linear branch is experimental evidence for the existence of flux flow domains. In the flux annihilation domain, an ac voltage component is induced by the continuous formation and decay of sine-Gordon breathers. Whitham's nonlinear WKB method is used to analyze the flux flow domains while the inverse scattering transform method is used as a qualitative guide to the study of breather formation in the flux annihilation domain.

AMS(MOS) Subject Classification - 35L05, 82A70

Key Words - Sine-Gordon equation, Kink, Breather, Whitham's method, Inverse scattering transform method, Fluxon annihilation

Work Unit No. 3 (Applications of Mathematics)

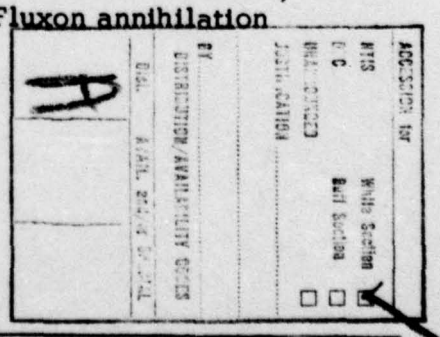

Sponsored by the United States Army under Contract No. DAAG29-75-C-0024
and by the National Science Foundation under Grant No. ENG 75-08492.

MAGNETIC FLUX ANNIHILATION IN A LARGE JOSEPHSON JUNCTION

Alwyn C. Scott

I. *INTRODUCTION*

The physical phenomenon to be discussed in this paper is the "displaced linear branch" in the volt-ampere characteristics of Josephson tunnel junctions having dimensions large compared with the Josephson penetration length (~ 0.1 mm). This effect was reported several years ago [1 - 3] and an explanation based on a continuous flow of magnetic flux quanta (fluxons) was suggested. Since that time, several striking advances have been made in the understanding of the analytic behavior exhibited by solutions of the underlying nonlinear partial differential equation, the sine-Gordon equation

$$\phi_{xx} - \phi_{tt} = \sin \phi \, . \tag{1.1}$$

Particularly important have been i) the development of an inverse scattering transform method (ISTM) for (1.1) [3 - 6], ii) the application of Whitham's method (WM), of slow perturbation of a single phase (periodic traveling wave) solution, to a dissipative version of (1.1) [7, 8]

$$\phi_{xx} - \phi_{tt} - \alpha\phi_t = \sin \phi, \tag{1.2}$$

iii) Ablowitz's discussions of the extension of Whitham's method to multiple phase (multiply periodic) solutions [9 - 12], and iv) demonstrations

Sponsored by the United States Army under Contract No. DAAG29-75-C-0024 and by the National Science Foundation under Grant No. ENG 75-08492.

that appropriate multiply periodic solutions assumed by Ablowitz do in fact exist for (1.1) [13 - 15]. The present discussion should be considered in context with previous efforts to apply the fruits of soliton theory to the problems of fluxon dynamics in large Josephson junctions [16, 17]. Such studies are of interest not only as an aid to understanding the volt-ampere characteristics of Josephson junctions [1 - 3, 18, 19], but also because the soliton properties of fluxons may make them useful as carriers of information [20 - 25].

The displaced linear branch was first observed on 1 mm. × 1 mm. crossed strip Josephson junctions as volt-ampere characteristics of the sort displayed in Figure 1. Above a critical current (I_c) for zero voltage (~ 1/2 ampere), the voltage (V) was found to increase linearly with the difference between current and critical current. Thus

$$\boxed{V = K(I-I_c)} \qquad (1.3)$$

where the constant of proportionality (K) is much less sensitive to temperature than the normal electron component of tunneling current. It was suggested [1] that the input power (VI) implied by (1.3) is carried by moving fluxons from the edges of the junction toward the center where it is given up in events of fluxon-antifluxon annihilation.

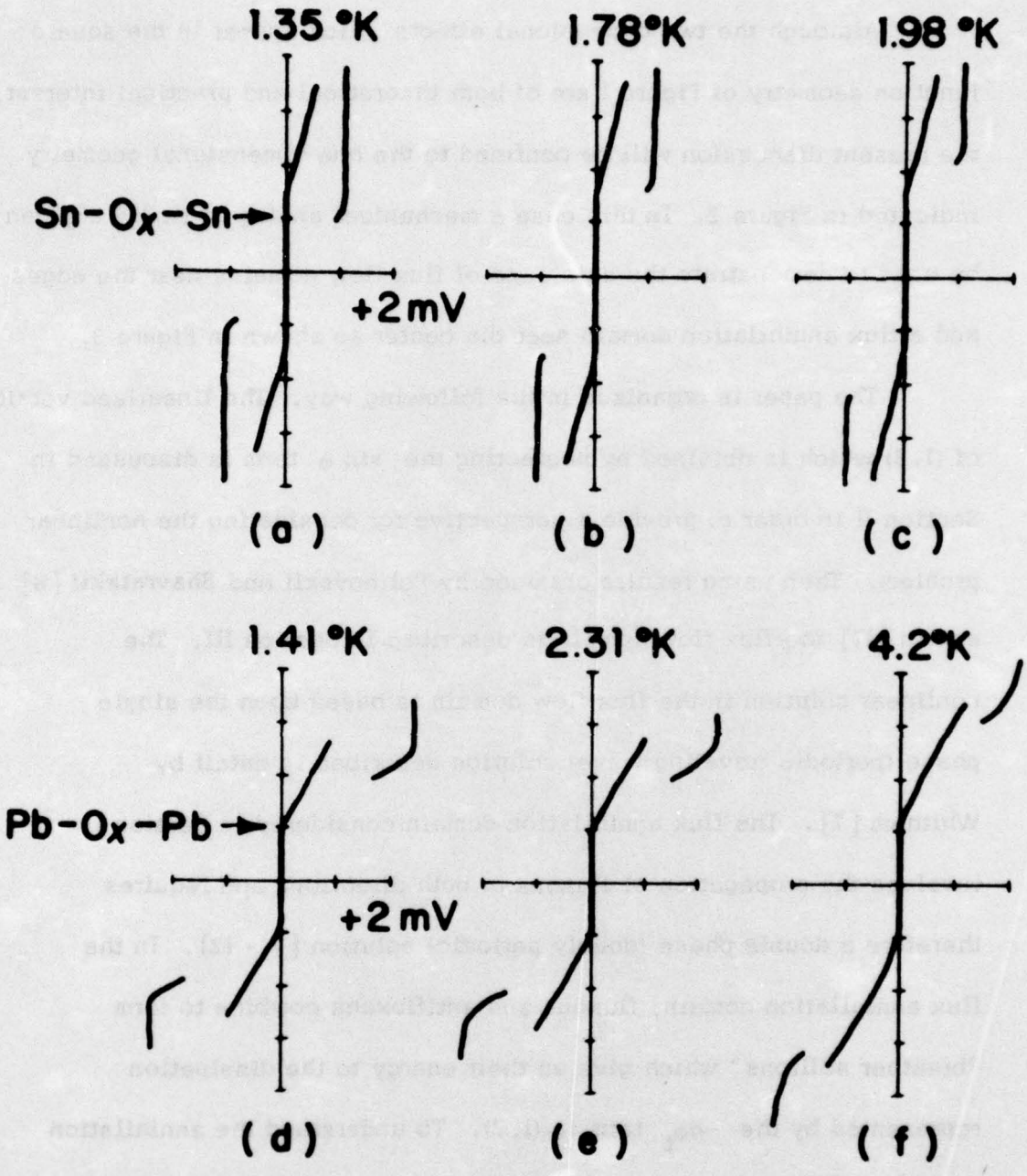

Figure 1. Volt-ampere characteristics of typical experimental junctions at various temperatures. (a), (b), and (c) are Sn-0_x-Sn, vertical: w00 mA/div, horizontal: 2 mV/div. (d), (e), and (f) Pb-0_x-Pb, vertical 500 mA/div, horizontal: 2mV/div.

Although the two dimensional effects which appear in the square junction geometry of Figure 1 are of both theoretical and practical interest, the present discussion will be confined to the one dimensional geometry indicated in Figure 2. In this case a mechanical analog of (1.2) [26] can be used to demonstrate the existence of flux flow domains near the edges and a flux annihilation domain near the center as shown in Figure 3.

The paper is organized in the following way. The linearized version of (1.2) which is obtained by neglecting the $\sin\phi$ term is discussed in Section II in order to provide a perspective for considering the nonlinear problem. Then using results obtained by Pelinovskii and Shavratzkii [8] and in [17] the flux flow domain is described in Section III. The nonlinear solution in the flux flow domain is based upon the single phase (periodic traveling wave) solution described in detail by Whitham [7]. The flux annihilation domain considered in Section IV involves the propagation of fluxons in both directions and requires therefore a double phase (doubly periodic) solution [9 - 12]. In the flux annihilation domain, fluxons and antifluxons combine to form "breather solitons" which give up their energy to the dissipation represented by the $-\alpha\phi_t$ term in (1.2). To understand the annihilation domain, it is important to appreciate the nature of breather solitons; thus two appendices are included which discuss (A) the structure of a

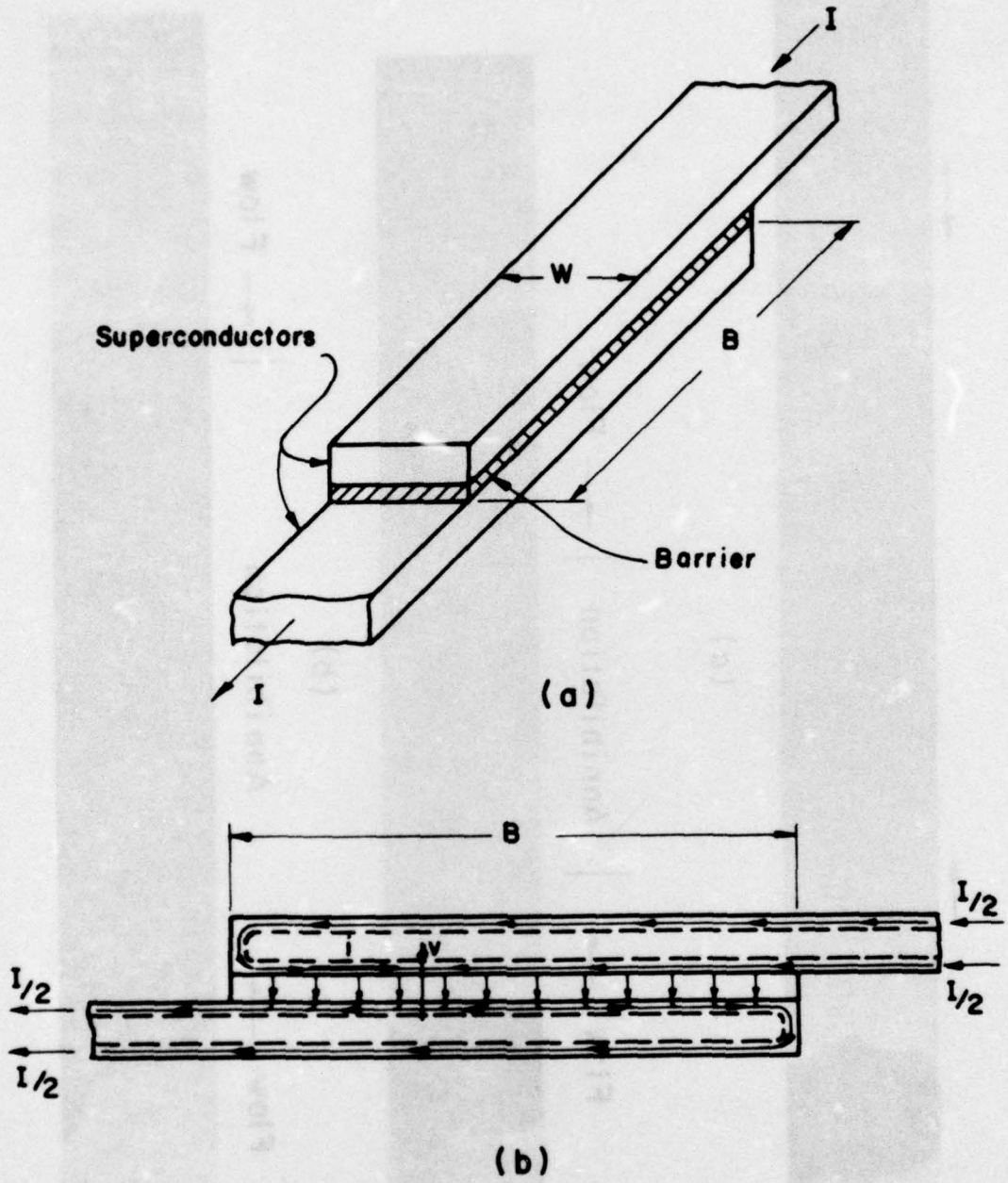

Figure 2. One dimensional geometry used for the theoretical analysis (not to scale). (a) perspective view, (b) section showing voltage v across insulating barrier and current i parallel to the barrier.

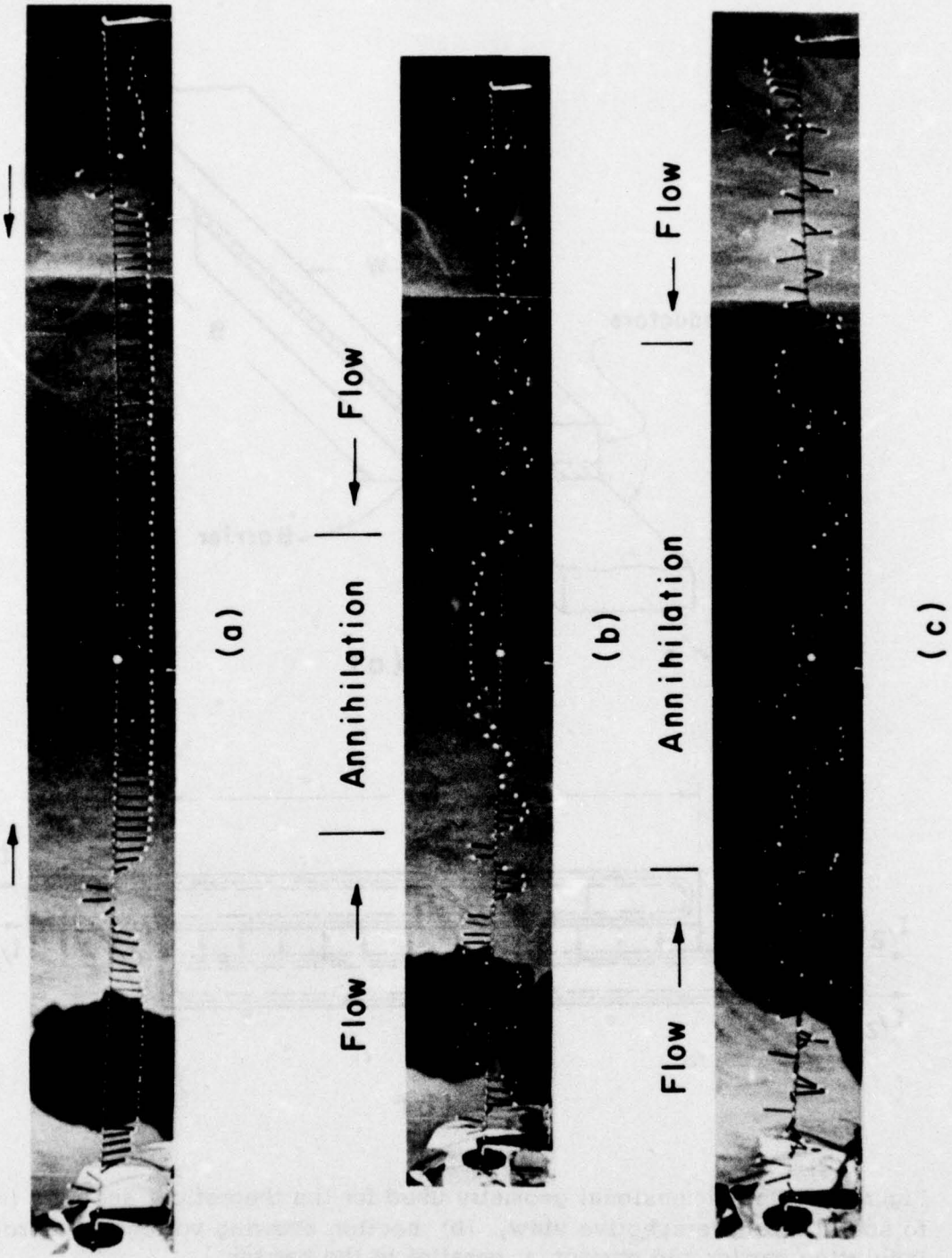

Figure 3. Kink flow domains and the kink annihilation (breather) domain on a mechanical analog of (1.2). (a) The crank is turned very slowly, (b) It is turned faster, (c) Faster still.

breather, and (B) the use of the inverse scattering transform method (ISTM) to study the generation of breathers through the interaction of double phase components. A third appendix (C) gives a summary account of single phase and double phase solutions for (1.1). The material in these appendices should be appreciated in order to follow the discussion of the main text. Finally we conclude with a review of the results which appear to be useful in interpreting currently available experimental data and some suggestions for future experiments.

The unnormalized form of (1.2) is

$$\Phi_{XX} - \ell g \Phi_{TT} - g\ell \Phi_T = j_0 \ell \sin(2\pi\Phi/\Phi_0) \qquad (1.4)$$

where

X is distance in the laboratory coordinate system,

T is time in the laboratory coordinate system,

$\Phi_T = V(X,T)$ is the voltage across the barrier,

$\Phi_X = -I(X,T)$ is the superconducting surface current flowing parallel to the barrier,

g is the shunt conductance through the barrier carried by (Giaever type [27]) normal electron tunneling per unit length,

ℓ is the inductance presented to the superconducting surface current per unit length,

c is the shunt capapacitance of the barrier per unit length,

and j_0 is the maximum (Josephson type [28]) superconducting electron tunneling through the barrier per unit length.

Thus

$$\Phi(X, T) = \int^{T} V(X, T')dT' \tag{1.5}$$

is the magnetic flux which has passed point X at time T. It is convenient to measure this in units of the magnetic flux quantum or fluxon

$$\begin{aligned} \Phi_0 &= h/2e \\ &= 2.067843 \times 10^{-15} \text{ volt-seconds.} \end{aligned} \tag{1.6}$$

If we define a Josephson length

$$\lambda_J \equiv \left[\frac{\Phi_0}{2\pi j_0 \ell}\right]^{1/2} \tag{1.7}$$

and note that the characteristic velocities of (1.4) are $\pm u_0$ where

$$u_0 = [\ell c]^{-1/2}, \tag{1.≡}$$

then (1.4) reduces to (1.2) with the normalizations

$$x = X/\lambda_J \tag{1.9}$$

$$t = u_0 T/\lambda_J \tag{1.10}$$

$$\phi = 2\pi\Phi/\Phi_0 \tag{1.11}$$

$$\alpha = g\ell u_0 \lambda_J . \tag{1.12}$$

Furthermore, if the shunt voltage across the barrier is normalized as

$$v = \frac{V}{\left[\frac{\Phi_0 j_0}{2\pi c}\right]^{1/2}} = \frac{V}{V_N} \tag{1.13}$$

and superconducting surface current as

$$i = \frac{I}{\left[\frac{\Phi_0 j_0}{2\pi \ell}\right]^{1/2}} = \frac{I}{I_N} , \tag{1.14}$$

then

$$\phi_t = v$$

$$\phi_x = -i . \tag{1.15a,b}$$

In this paper, we will be primarily concerned with an analysis of the normalized equation (1.2). A more detailed discussion of the approximations involved in obtaining (1.4) can be found in reference [17] together with some tables of experimentally measured values of the parameters.

II. THE LINEAR APPROXIMATION

We begin with a brief discussion of the equation

$$\phi_{xx} - \phi_{tt} - \alpha\phi_t = 0 \tag{2.1}$$

which is a linearization of (1.2) by neglecting the sine term. From (1.4) it can be seen that this is physically equivalent to assuming the coefficient of Josephson tunneling current (j_0) to be small. Equation (2.1) can also be written as the first order pde's

$$\begin{aligned} v_t + i_x &= -\alpha v \\ i_t + v_x &= 0 \end{aligned} \tag{2.2a,b}$$

where v and i are normalized shunt voltage and series current as defined in (1.13) through (1.15). The experimental situation indicated in Figure 2b can then be represented as in Figure 4a where the dimension $b = B/\lambda_J$. Physical symmetry and the boundary conditions require the current (i) to be zero at the center in Figure 4a. Thus we need consider only the half junction shown in Figure 4b with the boundary conditions

$$\begin{aligned} v(0, t) &= v_0 \\ i(b/2, t) &= 0. \end{aligned} \tag{2.3a,b}$$

If we assume v_0 = const. and seek steady state solutions, (2.2) implies

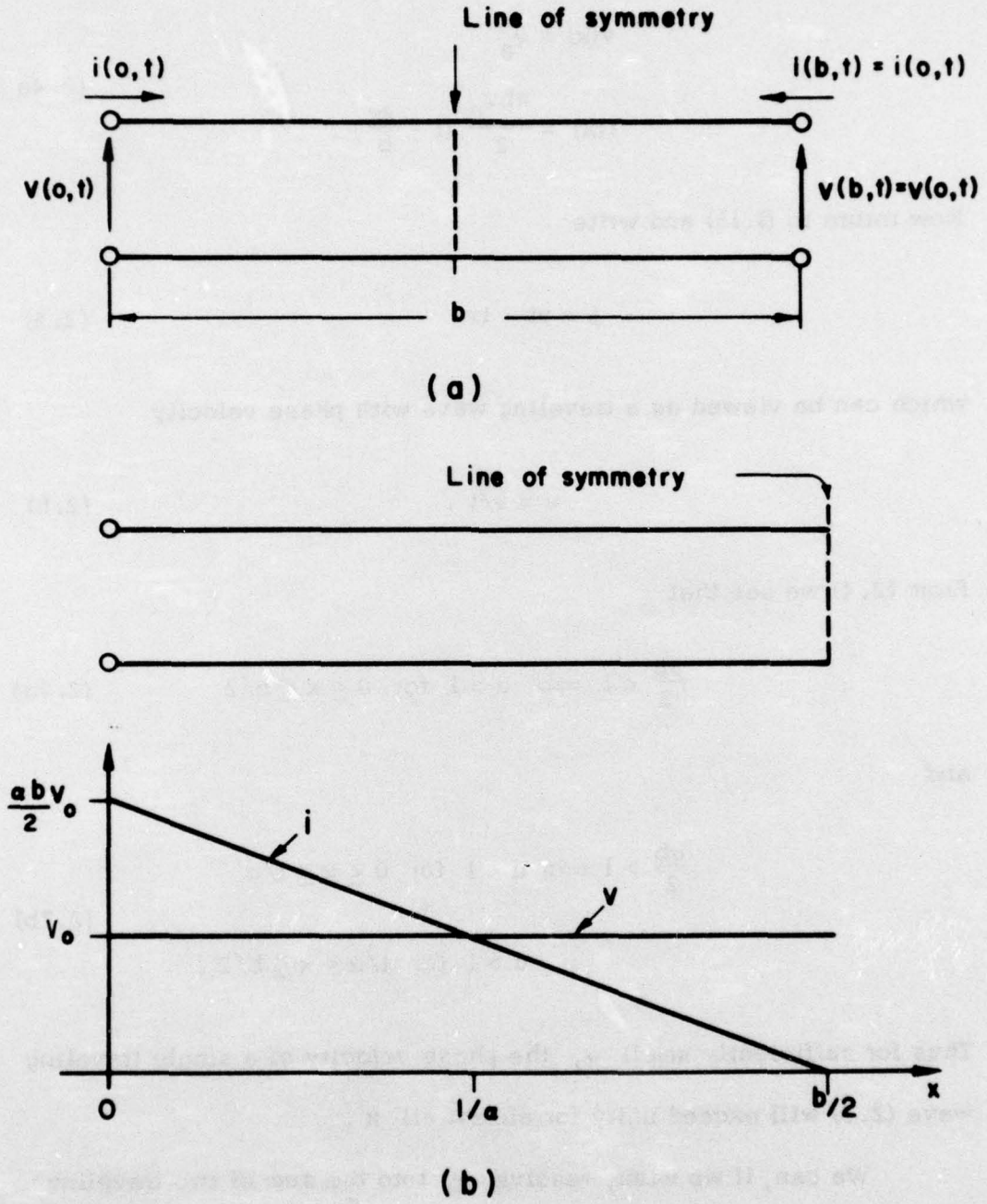

Figure 4. A linear approximation to the problem. State voltage v and current i .

$$v(x) = v_0$$

$$i(x) = \frac{\alpha b v_0}{2}\left(1 - \frac{2x}{b}\right) . \qquad (2.4a,b)$$

Now return to (1.15) and write

$$\phi = vt - ix \qquad (2.5)$$

which can be viewed as a traveling wave with phase velocity

$$u = v/i . \qquad (2.6)$$

From (2.4) we see that

$$\frac{\alpha b}{2} < 1 \implies u > 1 \text{ for } 0 \le x \le b/2 \qquad (2.7a)$$

and

$$\frac{\alpha b}{2} > 1 \implies u < 1 \text{ for } 0 \le x \le 1/\alpha$$

$$u > 1 \text{ for } 1/\alpha < x \le b/2 . \qquad (2.7b)$$

Thus for sufficiently small α, the phase velocity of a single traveling wave (2.5) will exceed unity for almost all x.

We can, if we wish, resolve ϕ into the sum of two traveling waves, one carrying flux to the right and the other carrying flux to the left. Then

$$\phi = (v_1 t - i_1 x) + (v_2 t + i_2 x) \ . \qquad (2.8)$$

where $v_1 + v_2 = v_0$ and $i_1 + i_2 = i(x)$. This resolution is not unique, but in anticipation of results to be obtained below for the nonlinear problem we suggest the following for the case $\alpha b/2 > 1$.

For $0 \leq x < 1/\alpha$ set $v_2 = 0$ and $i_2 = 0$ and take v_1 and i_1 to be the values given in (2.4). For $1/\alpha \leq x \leq b/2$ take

$$\begin{aligned} i_1 = v_1 &= \frac{v_0}{2} \left(\frac{b-1/\alpha-x}{b/2-1/\alpha}\right) \\ -i_2 = v_2 &= \frac{v_0}{2} \left(\frac{x-1/\alpha}{b/2-1/\alpha}\right) \ . \end{aligned} \qquad (2.9a,b)$$

Thus for $0 \leq x < 1/\alpha$ there is only a single traveling wave component and it has a phase velocity less than unity. For $1/\alpha < x \leq b/2$ there are two components and the phase velocity of each has a magnitude equal to unity.

III. THE FLUX FLOW DOMAIN

In this section we address ourselves to the nonlinear equation (1.2). Consider first a steady state solution. Then $\phi_{xx} = \sin \phi$ which is readily integrated to

$$\frac{1}{2}\phi_x^2 = E - \cos \phi \tag{3.1}$$

where E is a constant of integration. The conditions $\phi \to 0$ and $\phi_x \to 0$ at large x requires $E = 1$ whereupon

$$\phi_x = \pm 2 \sin \phi/2 .$$

From (1.15) i has maximum magnitude of $i_c = 2$ when $\phi(0) = \pi$. Thus the critical current (into <u>both</u> ends)

$$\boxed{I_c = 4\left[\frac{\Phi_0 j_0}{2\pi \ell}\right]^{1/2}} \tag{3.2}$$

is established below which the voltage $(v = \phi_t)$ is zero and above which flux must flow. This effect has been carefully investigated [29].

Suppose now that $i(0) > i_c$ $(I > I_c)$ so a steady state solution for (1.2) does not exist. As has been shown in reference [17], it is convenient to turn to Whitham's method of averaging for which it is supposed that the solution appears locally as a traveling wave of the form

$$\phi = \phi(\theta) \tag{3.3a,b}$$

$$\theta = \omega t - kx$$

where ω and k are allowed to be slowly varying functions of x and t. Then $\phi(\theta)$ is defined locally as the elliptic integral

$$\theta = \sqrt{k^2 - \omega^2} \int^{\phi} \frac{d\phi'}{\sqrt{2(E - \cos\phi')}} , \tag{3.4}$$

where we assume $E > 1$. Dynamic equations for the slow variation of k, ω and E with x and t are [7, 8, 17]

$$\begin{aligned} [\omega F'(E)F(E)]_t + [kF'(E)F(E)]_x &= -\alpha\omega F'(E)F(E) \\ k_t + \omega_x &= 0 . \end{aligned} \tag{3.5a,b}$$

The functions $F'(E)$ and $F(E)$ are complete elliptic integrals of the first and second kind respectively and defined as

$$\begin{aligned} F'(E) &\equiv \frac{1}{2\pi} \int_0^{2\pi} \frac{d\phi}{\sqrt{2(E - \cos\phi)}} \\ F(E) &= \frac{1}{2\pi} \int_0^{2\pi} \sqrt{2(E - \cos\phi)}\, d\phi \end{aligned} \tag{3.6a,b}$$

Note that in the large amplitude linear limit, $E \to \infty$,

$$\begin{aligned} F' &\to (2E)^{-1/2} \\ F &\to (2E)^{1/2} . \end{aligned} \tag{3.7a,b}$$

It is convenient to require that ϕ increase by 2π when θ does, whereupon k, ω and E are related by the nonlinear dispersion equation

$$k^2 - \omega^2 = [F'(E)]^{-2} . \qquad (3.8)$$

In the large amplitude linear limit ($E \gg 1$), the product

$$F'(E)F(E) \to 1$$

as is shown in Figure 5. Furthermore (3.4) and (3.8) imply

$$\phi \to \theta$$

so

$$v = \phi_t \to \theta_t = \omega$$
$$i = -\phi_x \to -\theta_x = k \qquad (3.9a,b)$$

and (3.5) approach the linear equations (2.2) which were considered in the previous section. Figure 5 indicates that this large amplitude linear limit is approached within a few percent for $E > 2$.

Suppose now that the current (i) is increased to the maximum zero voltage ($v = 0$) level. As i goes from 0^- to 0^+, the steady state current, $i(x)$, will jump from the solution of (3.1) (with $E = 1$) to a solution of (3.8) with $\omega = 0$ or

$$k = k_c = [F'(E_c)]^{-1} \qquad (3.10)$$

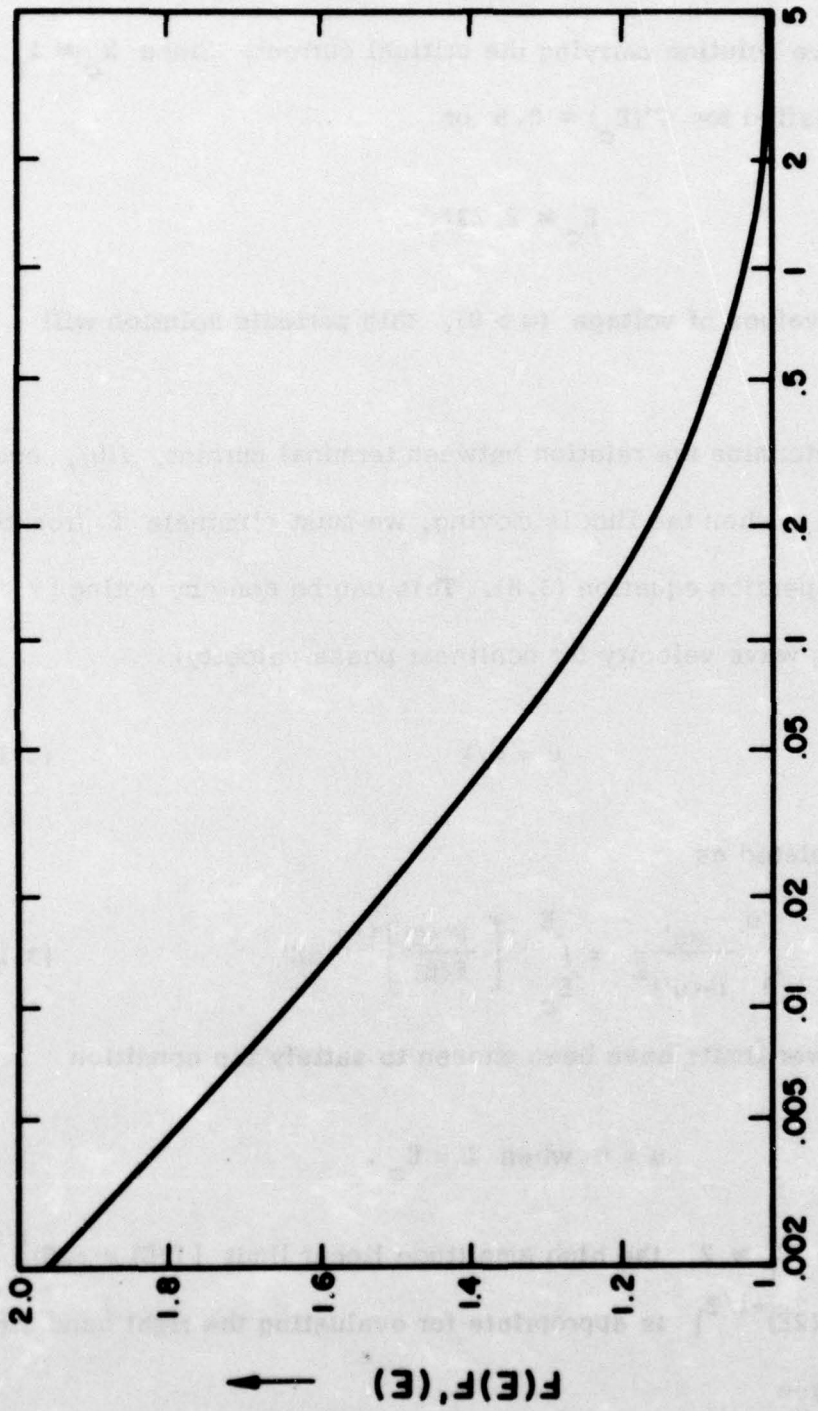

Figure 5 F(E) F'(E) vs. (E - 1).

where E_c is the critical value of the integration constant E for a traveling wave solution carrying the critical current. Since $k_c \approx i_c = 2$, (3.10) is satisfied for $F'(E_c) \approx 0.5$ or

$$E_c \approx 2.237.$$

For positive values of voltage ($\omega > 0$), this periodic solution will move.

To determine the relation between terminal current, $i(0)$, and voltage, $\omega(0)$, when the flux is moving, we must eliminate E from the nonlinear dispersion equation (3.8). This can be done by noting [7, 17] that traveling wave velocity (or nonlinear phase velocity)

$$u = \omega/k \tag{3.11}$$

and E are related as

$$\int_0^u \frac{du'}{1-(u')^2} = \int_{E_c}^{E} \left[-\frac{F'(E)}{F(E)}\right]^{1/2} dE' \tag{3.12}$$

where the lower limits have been chosen to satisfy the condition

$$u = 0 \text{ when } E = E_c .$$

Since $E_c \approx 2$, the high amplitude linear limit [$F(E) \approx (2E)^{1/2}$ and $F'(E) \approx (2E)^{-1/2}$] is appropriate for evaluating the right hand side of (3.12). Then

$$E(0) = E_c \left(\frac{1+u}{1-u}\right) \tag{3.13}$$

which upon substitution into (3.8) gives

$$\boxed{\omega(0) = k(0) - \sqrt{2E_c}} \quad . \tag{3.14a}$$

This is the equation for the displaced linear branch. Taking account of (3.9) and the normalizations in (1.13) and (1.14), it can be written

$$\boxed{V = \frac{1}{2}\sqrt{\frac{\ell}{c}}\ (I - I_c)} \quad . \tag{3.14b}$$

Thus the constant slope (K) which appears in (1.3) is equal to half the characteristic impedance of the linear operator in (1.2) [1], and the weak temperature dependence of this slope (see Figure 1) is readily appreciated.

Now let us consider how far such a steady state traveling wave solution can be extended into the junction. The assumption of steady state in (3.5b) implies

$$\omega = \text{const} \tag{3.15a}$$

and from (3.5a), k(x) must satisfy

$$[kFF']_x = -\alpha\omega FF' \ . \tag{3.15b}$$

Pelinovskii and Shavratzkii [8] have shown that there is a definite limit in x beyond which a single phase (periodic traveling wave) solution

of (3.15) does not exist. To see this consider the quantity kFF'. Using (3.8) it is seen to be

$$kFF' = F\sqrt{1 + \omega^2(F')^2} \tag{3.16}$$

which, for fixed ω, is a function of E with a minimum value ($E = E_{min}$) satisfying the condition

$$\omega^2\{[F'(E_{min})]^2 + F(E_{min})F''(E_{min})\} + 1 = 0. \tag{3.17}$$

The character of kFF' as a function of E and ω is displayed in Figure 6 and E_{min} vs. ω is plotted in Figure 7. When kFF' is equal to its minimum value, (3.15b) can no longer be satisfied because the right hand side requires that kFF' continue to decrease. It is only for the range of x for which $E > E_{min}$ that the steady state single phase solution can exist.

The value of x (say x_0) at which kFF' has fallen to its minimum value is an upper estimate for the boundary of the flux flow region. Equation (3.15) can be integrated with the boundary conditions

$$E = E(0) \quad \text{at} \quad x = 0$$

$$E = E_{min} \quad \text{at} \quad x = x_0$$

to obtain

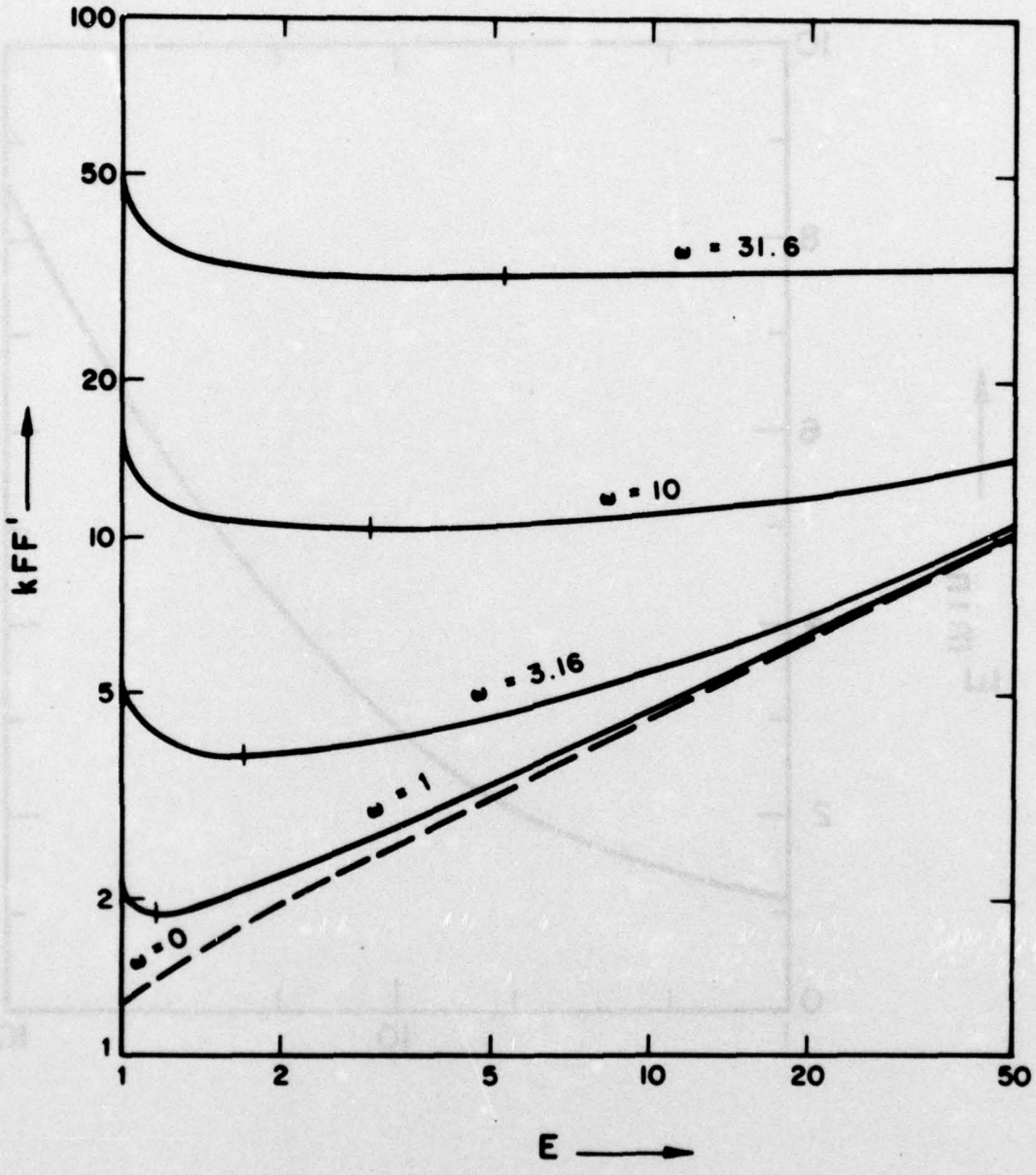

Figure 6 . k F(E) F'(E) vs. E .

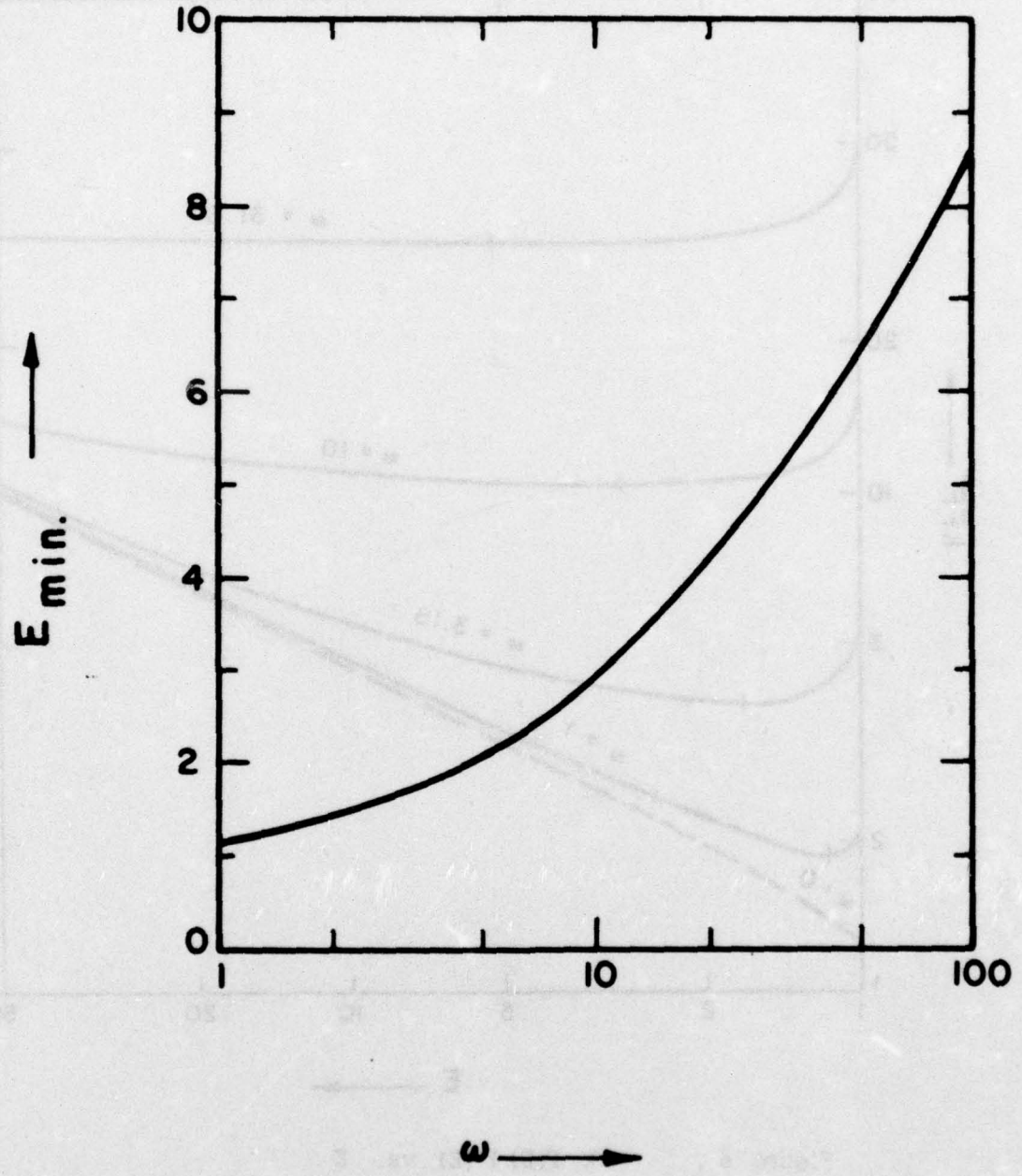

Figure 7. E_{min} vs. ω.

$$x_0 = \frac{1}{\alpha} \int_{E_{min}}^{E(0)} \left[\frac{1}{F} \sqrt{\frac{1}{\omega^2} + (F')^2} + \frac{\omega F''}{\sqrt{1 + \omega^2 (F')^2}} \right] dE \ . \quad (3.18)$$

where from (3.13) and (3.14)

$$E(0) = \omega\sqrt{2E_c} + E_c \ . \quad (3.19)$$

In the large amplitude linear limit (3.18) implies that $x_0 \to (2E_c)^{1/2}/\alpha\omega$ as $\omega \to \infty$, and $x_0 \to .607/\alpha\omega$ as $\omega \to 0$.

We are now prepared to calculate the power flowing across the boundaries of the flux flow region. In general $P(x) = \langle v(x)i(x) \rangle \approx \omega k(x)$ where the approximation improves for large E as indicated in (3.9). Taking the boundaries of the flux flow region as $x = 0$ and $x = x_0$ (see Figure 8), the power flowing in at $x = 0$ is

$$P(0) \doteq \omega k(0)$$
$$\doteq \omega^2 + \omega\sqrt{2E_c} \quad (3.20a,b)$$

where (3.14a) has been used to evaluate $k(0)$. In a similar way, the power flowing out at $x = x_0$ is

$$P(x_0) \doteq \omega k(x_0)$$
$$\doteq \omega\sqrt{\omega^2 + 2E_{min}} \quad (3.21a,b)$$

where (3.8) has been used to evaluate $k(x_0)$.

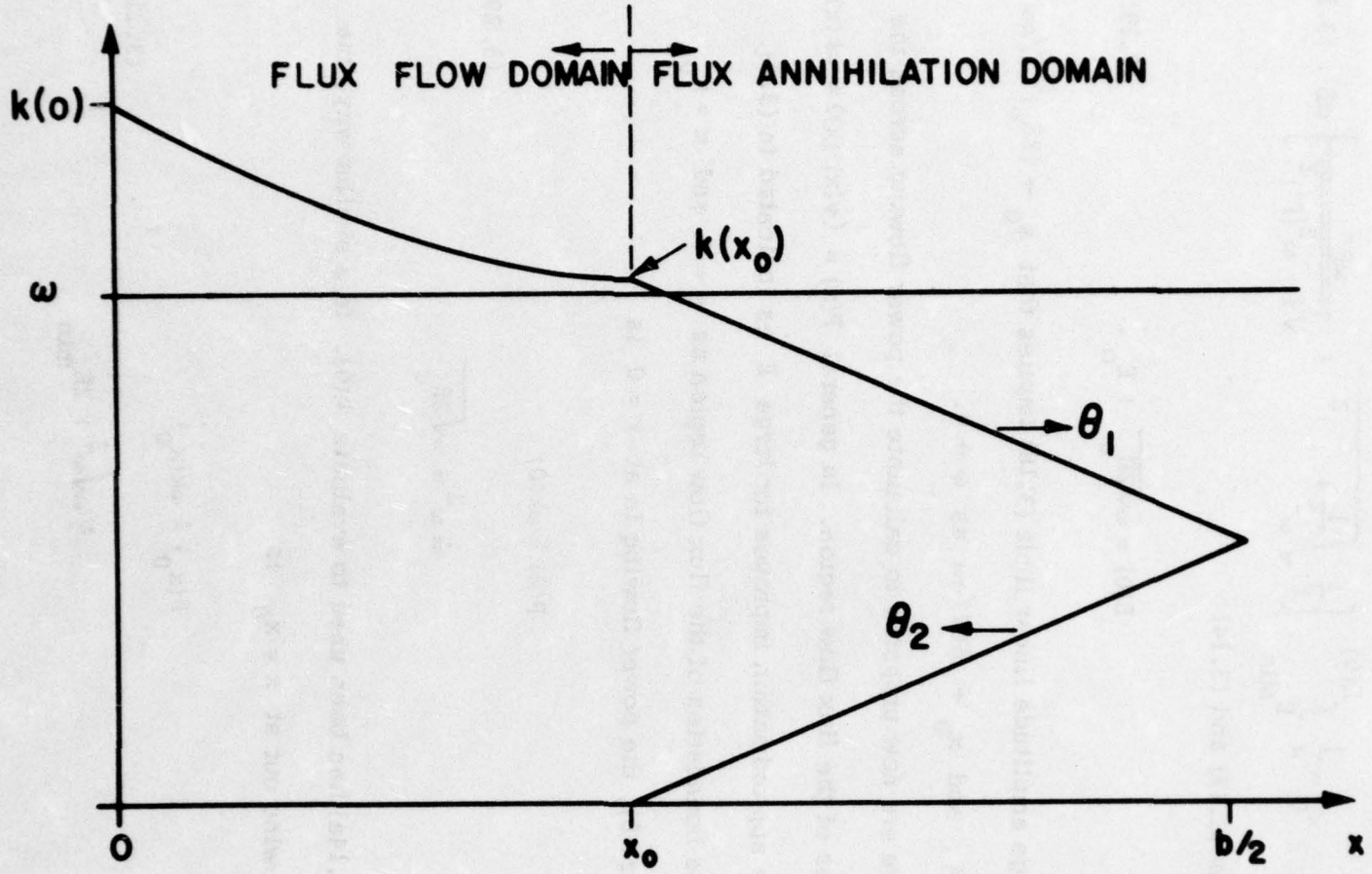

Figure 8. Steady state components of voltage (ω) and current (k) in the flux flow domains. In the flux annihilation domain, an approximation to the double phase solution is sketched.

If the assumption of steady state in the flux flow domain is correct, the difference between these incoming and outgoing powers must equal the d.c. dissipation. Thus we expect

$$P(0) - P(x_0) = \alpha\omega^2 x_0 \tag{3.22}$$

whereupon a second estimate for x_0 is

$$x_0 \doteq \frac{1}{\alpha}\left[1 + \frac{\sqrt{2E_c}}{\omega} - \sqrt{1 + \frac{2E_{min}}{\omega^2}}\right]. \tag{3.23}$$

We do not expect precise agreement between the values of x_0 calculated from (3.18) and (3.23) because the power flow estimates in (3.20a) and (3.21a) are not exact for smaller values of E.

However, as Figure 9 shows, the agreement is rather good. Equation (3.23) gives values for x_0 which are 7-10% higher than those calculated from (3.18) when ω lies between 1 and 2. Equation (3.23) is, of course, much more convenient than (3.18). For $\omega > 10$, the asymptotic expression

$$x_0 \sim \frac{\sqrt{2E_c}}{\alpha\omega} \tag{3.24}$$

is a reasonable approximation.

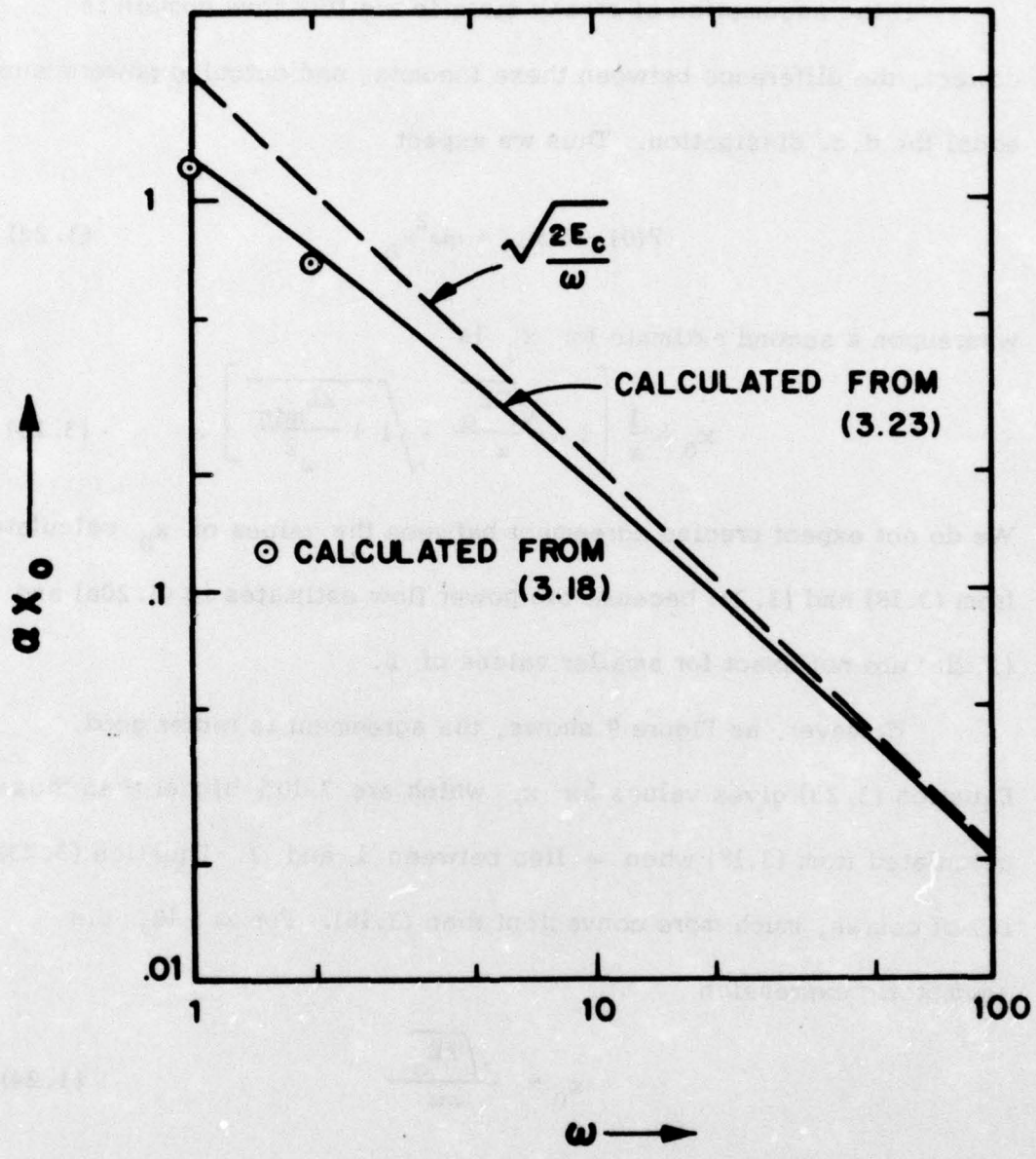

Figure 9. Maximum length of the flux flow domain (x_0) vs. voltage (ω).

IV. THE FLUX ANNIHILATION DOMAIN

Let us suppose that we have a large Josephson junction which exhibits a displaced linear branch (Figure 1) in the volt-ampere characteristics as is implied by (3.14). Assume further that α, b, ω and E_c are adjusted such that the relation

$$\frac{\alpha b}{2}\,\omega^2 = \omega(\omega + \sqrt{2E_c}) \tag{4.1}$$

holds. This relation says that the d.c. power into the junction (RHS) equals the d.c. power dissipated on the junction (LHS). If ω is increased above the value which satisfies (4.1), the LHS will be greater than the RHS and the displaced linear branch will not supply power to the junction at the rate it would be dissipated. Thus the value of ω which satisfies (4.1) is the "break voltage" ω_B (see Figure 10) above which the displaced linear branch will not continue. Figure 1 shows that such a break voltage is a characteristic feature of the displaced linear branch.

For $\omega_B \gg 1$, (4.1) implies that a necessary condition for observing a break in the displaced linear branch is

$$\frac{\alpha b}{2} \sim 1 \tag{4.2a}$$

or, in unnormalized units,

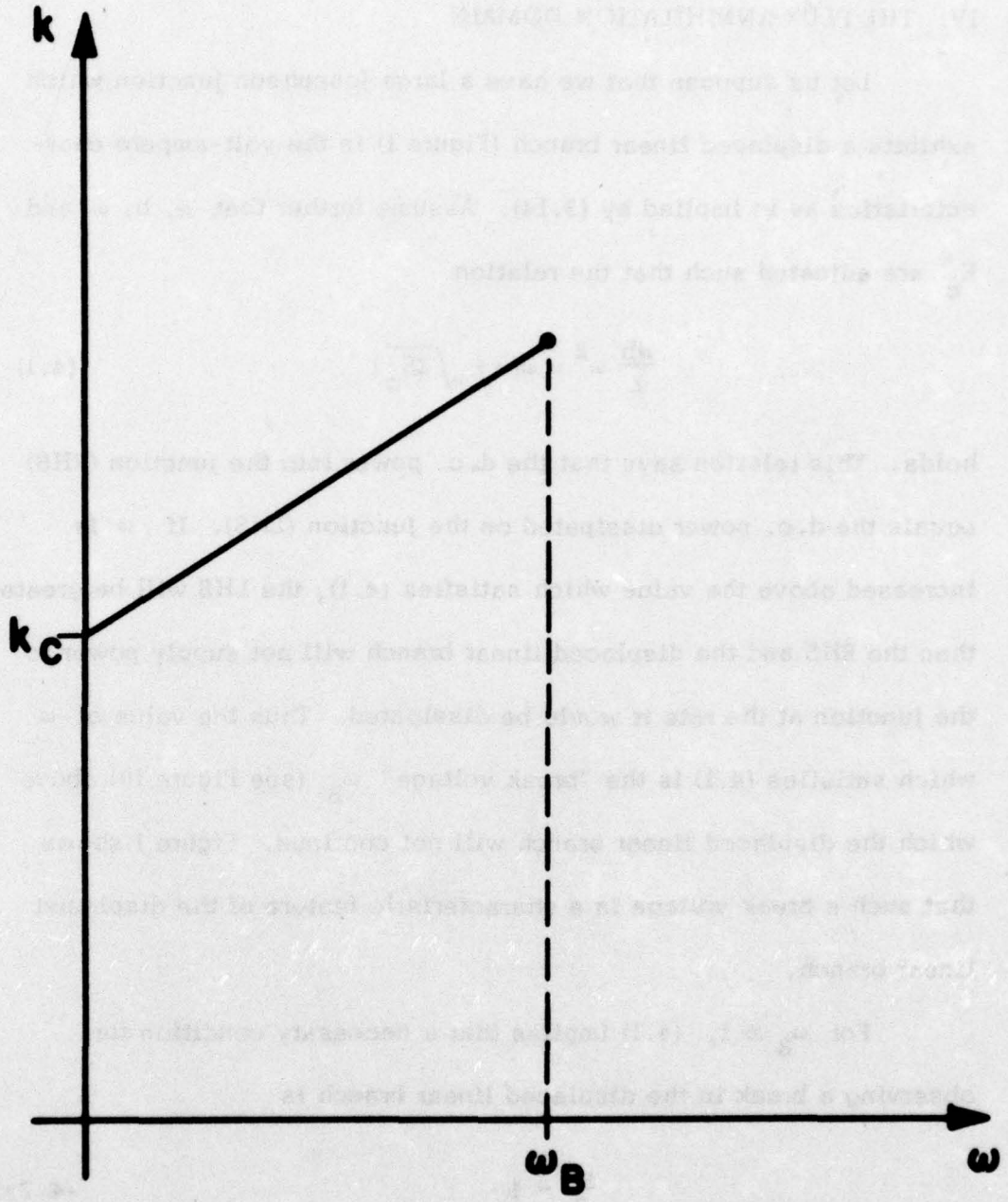

Figure 10. The break voltage (ω_B) in the displaced linear breathers.

$$gB \sim 2\sqrt{\frac{c}{l}} \quad . \tag{4.2b}$$

Now consider the difference between the power flowing into the flux annihilation domain, $P(x_0)$, and the d.c. power being dissipated in this domain

$$P_{dc} = \alpha\omega^2 (\frac{b}{2} - x_0) \quad . \tag{4.3}$$

Thus, from (3.21) and (3.23)

$$P(x_0) - P_{dc} = \omega^2 + \omega\sqrt{2E_c} - \alpha\omega^2 \frac{b}{2} \quad . \tag{4.4}$$

From (4.1) this difference is zero when $\omega = \omega_B$. For $\omega < \omega_B$, (4.4) indicates that the d.c. power flow into the flux annihilation domain is greater than the d.c. power dissipation in that domain. Thus for $\omega < \omega_B$ it is not possible to have a steady state (ω = const) in the flux annihilation domain. There must be an additional a.c. component of voltage to dissipate the power difference given by (4.4). The source for this a.c. voltage is the continuous creation of breather solitons near the center of the junction.

The dynamic activity in the flux annihilation domain is considerably more complex than in the flux flow domains. To get some qualitative appreciation for this activity we turn to the ideas developed in Section II and in the appendices. Consider first the problem of representing the

d.c. components or the time averages of v and i. Following Appendix C we assume a double phase solution

$$\phi(x, t) = \Phi(\theta_1, \theta_2) \tag{4.5}$$

with

$$\theta_1 \equiv \omega_1 t - k_1 x$$
$$\theta_2 = \omega_2 t - k_2 x . \tag{4.6a,b}$$

Then, motivated by (2.8), we try the simple form

$$\Phi(\theta_1, \theta_2) = \theta_1 + \theta_2 . \tag{4.7}$$

Equations (C-14) both become

$$(k_1 + k_2)_x = -\alpha(\omega_1 + \omega_2) \tag{4.8a}$$

and (C-6c, d) imply

$$\omega_1 + \omega_2 = \omega \text{ (a constant)}. \tag{4.8b}$$

The boundary condition $k_1(x_0) + k_2(x_0) = k(x_0)$ and (4.8a) implies

$$k_1 + k_2 = k(x_0) - \alpha\omega(x - x_0) . \tag{4.9}$$

The symmetry condition discussed in connection with Figure 4 requires $k_1(\frac{b}{2}) + k_2(\frac{b}{2}) = 0$, but from (4.9)

$$k_1(\tfrac{b}{2}) + k_2(\tfrac{b}{2}) = k(x_0) - \alpha\omega(\tfrac{b}{2} - x_0) \qquad (4.10)$$

$$= \omega + \sqrt{2E_c} - \frac{\alpha b}{2}\,\omega .$$

This is equal to zero only at the break voltage $\omega = \omega_B$. For $\omega < \omega_B$, the simple double phase function assumed in (4.7) cannot correctly represent the d.c. components. Some more versatile expression (probably using Riemann theta functions) will be required [13 - 15]. In the special case $\omega = \omega_B$, however, we can use (4.5) - (4.7) where

$$k_1(x) = k(x_0) - \omega(x-x_0) + \frac{k(x_0)}{2}\left(\frac{x - x_0}{b/2 - x_0}\right) \qquad (4.11a,b)$$

$$k_2(x) = -\frac{k(x_0)}{2}\left(\frac{x - x_0}{b/2 - x_0}\right) .$$

For $\omega_B - \omega \ll \omega_B$, (4.11) should be approximately correct.

Furthermore from (3.24) and (4.2a)

$$x_0 \sim \frac{\sqrt{2E_c}}{\omega}\,\frac{b}{2}$$

$$\ll \frac{b}{2}$$

so most of the junction will be occupied by the flux annihilation domain.

Also the rate at which kinks enter this domain at $x = x_0$ will be $\omega/2\pi$. Since each breather forms by coupling a kink entering from the left and an antikink from the right, the steady state rate of breather formation must equal $\omega/2\pi$.

Where in the flux annihilation domain will these breathers form ? To answer this question we can use the results of Appendix B as a qualitative guide. Just at the center of the junction, $\phi_x = 0$ and $\phi_t = \omega$. Thus, from (B-22), we expect the number of breathers formed per unit time and distance to be $\alpha\omega/2\pi$. Since the rate of rotation falls from a maximum at the center to zero at the edges of the flux annihilation domain, the net rate of breather formation should equal $\alpha b\omega/4\pi$. Then the condition (4.2a) implies a breather formation rate $\sim \omega/2\pi$.

Thus we have a fairly self consistent picture of breather formation for the case $\omega - \omega_B \ll \omega_B$. We expect the breathers to remain near the center of the junction because they are formed near the center of the junction as <u>stationary</u> breathers.

The case $\omega \ll \omega_B$ is much less well understood for several reasons.

i) The qualitative nature of the d.c. solution is not clear.

ii) From (4.4) the a.c. voltage is no longer a small fraction of the d.c. voltage.

iii) For $\omega \sim 1$, $x_0 \sim b/2$ and the flux annihilation domain becomes very narrow. In this case, the a.c. voltage is probably not confined to the flux annihilation domain.

Numerical studies of the case $\omega \ll \omega_B$ would be helpful in understanding these uncertain aspects. As far as the external observation of a displaced linear branch is concerned, however, all that is required is for a single phase (traveling wave) solution to be established near the edges of the junction.

V. CONCLUSIONS

Here an attempt will be made to draw together the somewhat tattered strands of the above discussion by indicating which results may have experimental significance and by suggesting some directions for future research.

1) Critical current.

From (3.2), the ciritical current (I_c) above which flux will begin to move is $4[\Phi_0 j_0/2\pi\ell]^{1/2}$. Since it is practical to compute j_0 and ℓ from independent measurements on a small junction [17], the ideal value for I_c can be compared with that actually observed on a large junction. Such a comparison is important because irregularities in the barrier thickness (d in Figure 2) may cause flux pinning and increase I_c above the value given by (3.2).

2) Slope of the displaced linear branch.

Equation (3.14b) indicates that the slope of the displaced linear branch should equal $2\sqrt{c/\ell}$ where the factor of two accounts for current flow into both ends of a long junction (see Figure 2b). This result confirms the suggestion made in [1]. Since c and ℓ can be independently measured on a small junction, this striking feature of the above theory for the displaced linear branch is always subject to direct experimental check.

3) Conditions for observing the displaced linear branch.

In (4.2) it was noted that the condition for observing a break in the displaced linear branch is $\alpha b \approx 2$ or, in unnormalized units, $gB \approx 2\sqrt{c/\ell}$. If $\alpha b \gg 2$, the Josephson current becomes a small portion of the total current, and the situation reduces to the linear problem studied in Section II. If, on the other hand, $\alpha b \ll 2$, the junction becomes a resonant electromagnetic structure, and the step structure observed by Fiske [30-33] will dominate the volt-ampere characteristic. Thus the condition

$$\frac{\alpha b}{2} \sim 1 \qquad (5.1a,b)$$

or

$$gB \sim 2\sqrt{c/\ell}$$

also determines the range of experimental parameters for which the displaced linear branch should be unambiguously observed.

4) Numerical studies.

It was assumed, in the discussions of Sections III and IV, that the a.c. voltage associated with the decay of breather solitons is confined to the flux annihilation domain and does not "leak out" into the flux flow domain. This assumption seems plausible because stationary breathers are generated at the center of the junction and it is confirmed in a

rough way by observations on the mechanical model as shown in Figure 3. But it would be comforting to have a direct numerical test of this picture. An appropriate problem would be integration of (1.2) with end conditions

$$\omega(0, t) = \omega(b, t) = 0 \quad \text{for} \quad t < 0$$

$$= v \quad \text{for} \quad t > 0$$

and with $\alpha b = 2$, $\alpha = 0.1, 0.01, 0.001$, and $v = 1, 10, 100$. An asymptotic form of the dynamic activity should be sought as $t \to \infty$.

5) Experiments with light sensitive junctions.

Barone et al. [34] have recently demonstrated that properly prepared Pb - CdS - In junctions can be changed from "small" ($b < 1$) to "large" ($b > 1$) by ordinary optical illumination. This change occurs because the Josephson tunneling is increased and therefore λ_J is decreased under illumination. An increase in the Josephson tunneling should correspond to an increase in the normal electron (Giaever) tunneling and therefore an increase in α. Thus αb should be an even more sensitive function of illumination than b. Indeed, from (5.16), αb is directly proportional to the Giaver tunneling density.

Thus it may be possible to experimentally observe a transition from "Fiske steps" on a "small" junction to flux flow on a "large" junction as the illumination level is increased.

APPENDIX A: STRUCTURE OF A BREATHER

1. Classical structure

Consider the sine-Gordon equation in characteristic coordinates

$$\phi_{\xi\tau} = \sin\phi \qquad \text{(A-1}$$

which is equivalent to (1.1) under the independent variable transformation

$$\xi = \frac{1}{2}(x-t)$$

$$\tau = \frac{1}{2}(x+t)\ . \qquad \text{(A-2a,b)}$$

If $\phi_{n-1}(\xi,\tau)$ is a solution of (A-1), it is easily shown that $\phi_n(\xi,\tau)$ which satisfies

$$(\phi_n-\phi_{n-1})_\xi = 4i\gamma \sin\left(\frac{\phi_n+\phi_{n-1}}{2}\right)$$

$$(\phi_n+\phi_{n-1})_\tau = -\frac{i}{\gamma}\sin\left(\frac{\phi_n-\phi_{n-1}}{2}\right) \qquad \text{(A-3a,b)}$$

is also a solution [35]. This is called a Bäcklund transform which generates a new solution from a known (old) solution; by repeated application a hierarchy of solutions can be obtained. If $i\gamma_j$ is real, an additional kink or soliton will be introduced with the asymptotic form

$$\phi_j = 4\tan^{-1}[\exp(2i\gamma_j\xi - i\tau/2\gamma_j)] \qquad \text{(A-4)}$$

and velocity in the laboratory (x, t) frame [17]

$$u_j = \frac{4\gamma_j + 1}{4\gamma_j - 1} \quad . \tag{A-5}$$

As George Lamb has suggested [36], a convenient way to generate a breather solution to (1.1) is to perform two Bäcklund transforms with complex γ's and

$$\gamma_1 = -\gamma_2^* \, . \tag{A-6}$$

Such a solution, ϕ_B, is given by [16, 35, 36]

$$\tan \frac{\phi_B}{4} = \left(\frac{\gamma - \gamma^*}{\gamma + \gamma^*} \right) \tan \left(\frac{\phi_1 - \phi_2}{4} \right) \tag{A-7}$$

where ϕ_1 and ϕ_2 have the Gudermannian form indicated in (A-4). Thus in the laboratory (x, t) frame a <u>breather soliton</u> has the form

$$\phi_B = 4 \tan^{-1} \left\{ \left(\frac{\gamma - \gamma^*}{\gamma + \gamma^*} \right) \frac{\exp[\, i(\gamma - \frac{1}{4\gamma})x - i(\gamma + \frac{1}{4\gamma})t] - \exp[\, -i(\gamma^* - \frac{1}{4\gamma^*})x + i(\gamma^* + \frac{1}{4\gamma^*})t]}{1 + \exp[\, i(\gamma - \gamma^* - \frac{1}{4\gamma} + \frac{1}{4\gamma^*})x + i(-\gamma + \gamma^* - \frac{1}{4\gamma} + \frac{1}{4\gamma^*})t]} \right\} . \tag{A-8}$$

Upon examination of (A-8), the following points will be noted.

i) As $\gamma \to$ a pure imaginary #, $\phi_B \to 2\pi$ and the breather disassociates into a kink-antikink pair.

ii) As $\gamma \to$ a real #, $\phi_B \to 0$ and is proportional to $\sin(kx - \omega t)$ where $k = \gamma - 1/4\gamma$, $\omega = \gamma + 1/4\gamma$ and $\omega^2 = 1 + k^2$.

iii) The envelope of the breather is determined by the denominator in (A-8). The envelope velocity

$$u_e = \frac{\gamma + \frac{1}{4\gamma} - \gamma^* - \frac{1}{4\gamma^*}}{\gamma - \frac{1}{4\gamma} - \gamma^* + \frac{1}{4\gamma^*}} \qquad \text{(A-9)}$$

is positive for $|\gamma| > 1/2$ and negative for $|\gamma| < 1/2$. Thus the condition for a <u>stationary breather</u> is

$$|\gamma| = \frac{1}{2} . \qquad \text{(A-10)}$$

In terms of an angle parameter (β) which relaxes from $\frac{\pi}{2} \to 0$ as two kinds decay into a stationary breather of zero energy, (see Figure 11) a stationary breather takes the form

$$\phi_B = 4 \tan^{-1} \{\tan \beta \sin[(\cos \beta)t] \operatorname{sech}[(\sin \beta)x]\} . \qquad \text{(A-11)}$$

The rest energy of a breather can be calculated as the total energy of a stationary breather from the Hamiltonian density

$$H = \frac{1}{2}\phi_x^2 + \frac{1}{2}\phi_t^2 + 1 - \cos \phi \qquad \text{(A-12)}$$

corresponding to (1.1). At $t = 0$, (A-11) reduces to $\phi_B(x,0) = 0$; so $H = \frac{1}{2}\phi_{B,t}^2(x,0)$ and the total energy

$$U_B = \int_{-\infty}^{\infty} H dx$$

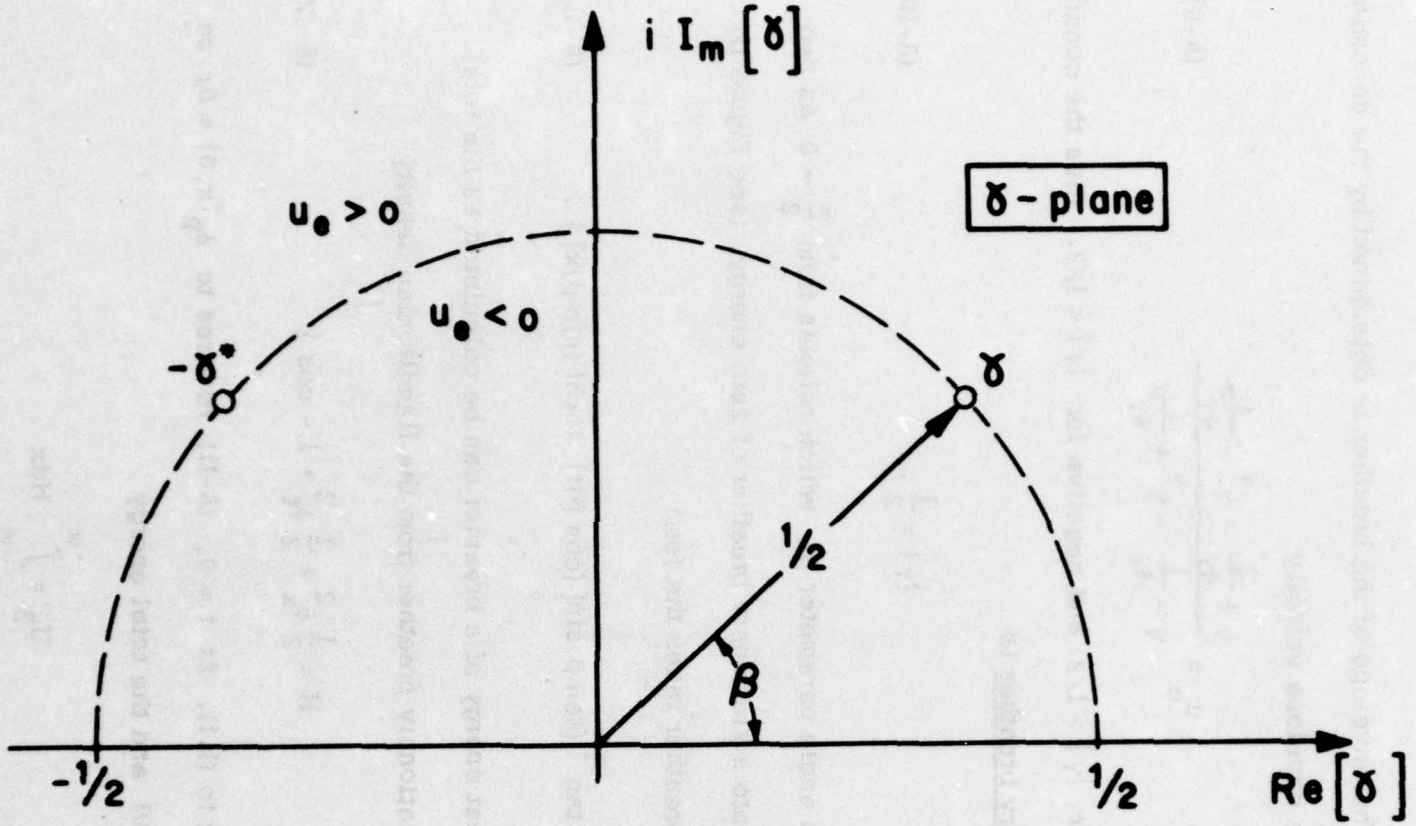

Figure 11. Locus of eigenvalues for stationary breathers.

or

$$U_B = 16 \sin \beta \ . \tag{A-13}$$

When β reaches $\pi/2$, the breather disassociates into two kinks of the form (A-4), so the energy of a kink is

$$U_k = 8 \ . \tag{A-14}$$

2. Quantum structure

Fadeev [37, 38] and Dashen, Hasslacher and Neveu [39] have carried through an exact quantization of the breather soliton described by (A-11). The discrete energy levels were found to be

$$U_n = 2\tilde{U}_k \sin\left[\frac{\hbar\omega_J}{2\tilde{U}_k}\right](n + 1/2) \tag{A-13}$$

where $\tilde{U}_k$ is the unnormalized energy of a kink (fluxon), $\hbar$ is Planck's constant divided by 2π and

$$\omega_J = u_0/\lambda_J \tag{A-14}$$

is the Josephson frequency which was used in (1.10) to normalize the time scale. There is correspondence between the classical frequency (cos β) in (A-11) and the frequency for emission or absorption in (A-13) if

$$\beta = \frac{\omega_J}{2\tilde{U}_k}(n + 1/2) \ . \tag{A-15}$$

Thus the allowed quantum states for a stationary breather are evenly spaced on the circle $|\gamma| = 1/2$ (see Figure 11). Quantum effects should become important in predicting the dynamics of a breather if the number of these states is not large compared with unity. To evaluate this situation we note that in unnormalized units

$$\tilde{U}_k = 8cV_N^2\lambda_J = \frac{4}{\pi}\Phi_0 j_0 \lambda_J \qquad \text{(A-16)}$$

and turn to the parameters measured on the Josephson transmission lines discussed in reference [17]. From (A-14) the total number of levels is

$$N = \frac{4\tilde{U}_k}{\pi\hbar\omega_J} \qquad \text{(A-17)}$$

Table I. Estimates of Quantum Structure for Breathers

	N53C	N25L	
λ_j	2.63×10^{-4}	1.27×10^{-3}	meter
ω_J	6.69×10^{10}	1.81×10^{10}	rad/sec.
j_0	1.9	.097	amp/meter
J_0	1.22	.062	amp/CM^2
U_k	13.1×10^{-19}	3.24×10^{-19}	joules
$N(=4\tilde{U}_k/\pi\hbar\omega_J)$	2.37×10^5	2.16×10^5	----

From the last entry in Table I it is clear that the number of quantum levels is so large that classical dynamics should be sufficiently

accurate for the description of these particular Josephson transmission lines. As for other structures it should be noted that $N \propto j_0 \lambda_J^2$ or

$$N \propto W \tag{A-18}$$

where W is the width of the transmission line (see Figure 2a). If W were decreased by two orders of magnitude (from 64 microns to 0.64 micron), quantum corrections would still be of minor importance. This is in accord with a previous estimate of the need for quantum corrections in a point contact Josephson junction [40].

APPENDIX B: A COHERENT BREATHER GAS FROM ROTATING INITIAL CONDITIONS

Here we use the inverse scattering transform method for the sine-Gordon equation (1.1), which was discovered by Ablowitz, Kamp, Newell and Segur [4], to see how a breather gas can be generated. In laboratory coordinates the equations for evolution of the scattering variable $\psi = (\psi_1, \psi_2)$ are

$$\psi_{1,x} = -\frac{i}{2}\left(\gamma - \frac{1}{4\gamma}\cos\phi\right)\psi_1 + \frac{1}{2}\left[\frac{i}{4\gamma}\sin\phi - \frac{1}{2}(\phi_x - \phi_t)\right]\psi_2$$

$$\psi_{2,x} = \frac{1}{2}\left[\frac{i}{4\gamma}\sin\phi + \frac{1}{2}(\phi_x - \phi_t)\right]\psi_1 + \frac{i}{2}\left(\gamma - \frac{1}{4\gamma}\cos\phi\right)\psi_2 \qquad \text{(B-1a, b)}$$

and

$$\psi_{1,t} = \frac{i}{2}\left(\gamma + \frac{1}{4\gamma}\cos\phi\right)\psi_1 + \frac{1}{2}\left[\frac{i}{4\gamma}\sin\phi + \frac{1}{2}(\phi_x - \phi_t)\right]\psi_2$$

$$\psi_{2,t} = \frac{1}{2}\left[\frac{i}{4\gamma}\sin\gamma - \frac{1}{2}(\phi_x - \phi_t)\right]\psi_1 - \frac{i}{2}\left(\gamma + \frac{1}{4\gamma}\cos\phi\right)\psi_2 \; . \qquad \text{(B-2a, b)}$$

These equations are closely related to the Bäcklund transform equations (A-3) [5, 41] for which we noted that a purely imaginary γ introduced a kink or soliton and a pair $(\gamma, -\gamma^*)$ introduced a breather into the total solution.

The application of such scattering equations to compute the evolution of nonlinear waves from specified initial conditions has been discussed in detail [5, 17]. Here I will merely sketch a particular calculations of interest to our study of the flux annihilation domain in Section IV.

Refer to Figure 12 and consider the following initial conditions on $\phi(x, t)$ which is to be a solution of (1.1)

$$\phi(x, 0) = 0$$

$$\phi_t(x, 0) = 0 \quad \text{for} \quad |x| > p \qquad \text{(B-3a, b)}$$

$$= V \quad \text{for} \quad |x| \leq p \ .$$

A scattering problem is defined as indicated where ψ_i and ψ_r are the asymptotic incident and reflected waves in Region (3) and ψ_t is the asymptotic transmitted wave in Region (1). Since ψ obeys (B-1, 2) in all regions, the asymptotic forms indicated in Figure 12 follow directly from assuming $\phi \to 0$ as $|x| \to \infty$ and writing

$$\gamma' = \gamma - \frac{1}{4\gamma} \ . \qquad \text{(B-4)}$$

Bound states of the scattering problem require $a(\gamma') = 0$ and $\text{Im}(\gamma') > 0$. The corresponding bound state eigenvalues represent the kinks and breathers to be found in the evolution of $\phi(x,t)$. It is easily shown that under (B-4) the upper (lower) half of the γ plane maps to the upper (lower) half of the γ'-plane; thus the condition for a bound state is the same in laboratory (x,t) coordinates as in the characteristic (ξ, τ) coordinates usually used to discuss the ISTM for the sine-Gordon equation.

Since the bound state eigenvalues are independent of time, they can be determined from the initial conditions (B-3) at $t = 0$.

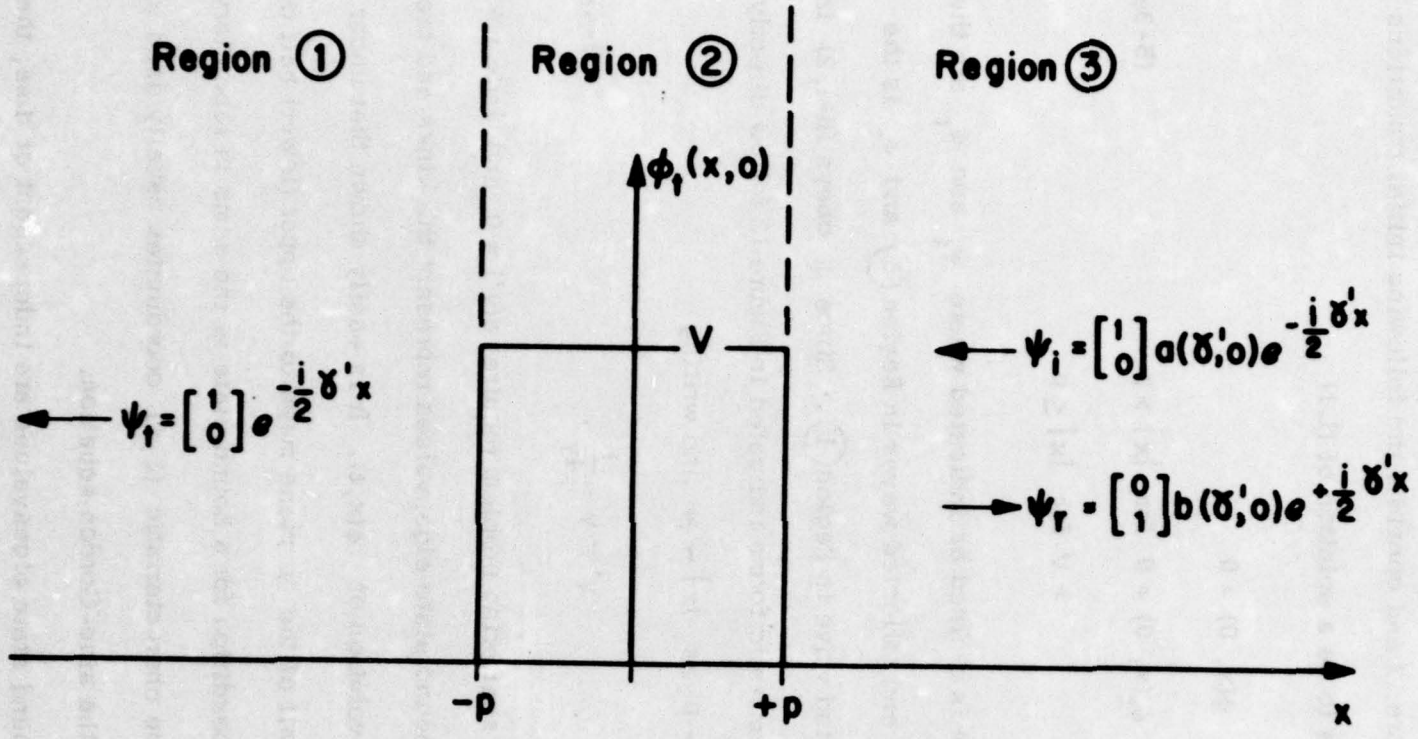

Figure 12. The scattering problem at $t = 0$ for rotating initial conditions.

In Region (1)

$$\psi_1 = e^{-\frac{i}{2}\gamma' x}$$

$$\psi_2 = 0 \,. \tag{B-5a, b}$$

In Region (2) (Proceeding as in [17])

$$\psi = \begin{bmatrix} (\cos mx - \frac{i\gamma'}{2m} \sin mx) & \frac{V}{4m} \sin mx \\ -\frac{V}{4m} \sin mx & (\cos mx + \frac{i\gamma'}{2m} \sin mx) \end{bmatrix} \times \begin{bmatrix} \psi_{10} \\ \psi_{20} \end{bmatrix} \tag{B-6}$$

where

$$(2m)^2 \equiv (\gamma')^2 + (\frac{V}{2})^2 \,. \tag{B-7}$$

The boundary conditions at $x = -p$ determine the constants ψ_{10} and ψ_{20} as

$$\psi_{10} = (\cos mp - \frac{i\gamma'}{m} \sin mp) e^{\frac{i}{2}\gamma' p}$$

$$\psi_{20} = (-\frac{V}{4m} \sin mp) e^{\frac{i}{2}\gamma' p} \,. \tag{B-8a, b}$$

Then the boundary conditions at $x = +p$ determine

$$a(\gamma', 0) = e^{i\gamma' p} [(\cos mp - \frac{i\gamma'}{2m} \sin mp)^2 - (\frac{V}{4m})^2 \sin^2 mp] \tag{B-9}$$

as the incident wave amplitude at time $t = 0$.

The bound states are determined by the condition $a(\gamma', 0) = 0$ which can be expressed as

$$\cot 2mp = \frac{i\gamma'}{2m} \quad . \tag{B-10}$$

This condition together with (B-7) is just the pair of equations studied previously in connection with the problem of fluxon propagation [17]. The only difference is that γ has been replaced by γ' which is related to γ by (B-4). Thus we can immediately state that all the roots of (B-10) which lie in the upper half of the γ'-plane lie on the imaginary axis, and the construction of Figure 11 in reference [17] will find them. In particular we note that $2m_n p \approx n\pi$ for most of the roots, so from (B-7)

$$\gamma_n' \approx \frac{i}{p} \sqrt{\left(\frac{Vp}{2}\right)^2 - (n\pi)^2} \quad . \tag{B-11}$$

To see which of these roots correspond to breathers we must return to the γ-plane and use the results of the preceding appendix. First we write (B-4) in the form

$$\gamma = \frac{1}{2}\left[\gamma' \pm \sqrt{(\gamma')^2 + 1}\right] . \tag{B-12}$$

As V is increased from zero, threshold levels (V_n) are reached at which new zeros of $a(\gamma', 0)$ appear in the upper half of the γ'-plane. Each enters at the origin and moves up the imaginary axis of the γ'-plane.

From (B-12) a corresponding pair of zeros enters the γ-plane at $\gamma = \pm 1/2$ and move up the circle $|\gamma| = 1/2$ indicated in Figure 11. Thus stationary breathers are generated just above threshold by the initial conditions (B-3). From the construction in Figure 11 of [17], it is easily seen that the threshold condition for the n^{th} breather pair is

$$V_n = (2n-1)\pi/p \ . \tag{B-13}$$

From (B-11) we note that as $p \to \infty$ most of the zeros lie at $\gamma' = iV/2$. For $V < 2$, (B-12) indicates that they lie on the circle $|\gamma| = 1/2$ in Figure 11 and cluster at

$$\beta = \sin^{-1}(V/2) \ . \tag{B-14}$$

As $p \to \infty$ and $V < 2$ in Figure 12, we have $\phi_{xx} \to 0$ everywhere whereupon (1.1) reduces to the pendulum equation

$$\phi_{tt} = \sin \phi \ . \tag{B-15}$$

This extended oscillation may be viewed as "gas" of a large number of synchronized or coherent breathers.

It is interesting to compare the energy of this coherent state with the total input energy U_0. From the Hamiltonian density (A-12) and the initial conditions (B-3), this energy is

$$U_0 = V^2 P \tag{B-16}$$

which can be portioned between i) kinks (of which there are none when $V < 2$), ii) breathers and iii) radiation. Since these three energy components are positive definite [38], the energy of the N breathers

$$U_{NB} \leq U_0. \tag{B-17}$$

An upper bound on U_{NB} is obtained by noting that the approximation (B-11) underestimates $|\gamma_n'|$ so

$$|\gamma_n'| > \frac{V}{2}\sqrt{1 - (\frac{2n\pi}{Vp})^2} \tag{B-18}$$

and from (B-14) the energy of the n^{th} breather

$$U_{NB} > 8V\sqrt{1 - (\frac{2n\pi}{Vp})^2} \quad . \tag{B-19}$$

From (B-13) the number of breathers (N) is the largest integer less than

$$\frac{Vp+\pi}{2\pi} \quad .$$

Thus there are no breathers, and no breather energy, when

$$Vp < \pi.$$

In general the total breather energy

$$U_{NB} > \sum_{n=1}^{N} 8V\sqrt{1- (\frac{2n\pi}{Vp})^2} \quad . \tag{B-20}$$

For

$$Vp \gg 2\pi$$

the right hand side of (B-20) can be approximated by the integral

$$\frac{4}{\pi} V^2 p \int_0^1 \sqrt{1-y^2}\, dy = V^2 p \, .$$

Thus (B-20) and (B-17) together imply

$$U_{NB} \to U_0$$

as $p \to \infty$ with $V < 2$. For a number of breathers large compared with unity, essentially all the input energy goes into the breathers. If $Vp = 2\pi N$, (B-20) implies U_{NB}/U_0 is greater than 55% for $N = 2$, greater than 71% for $N = 3$ and greater than 79% for $N = 4$.

Finally let us suppose that

$$V \gg 2$$

and we are interested in the behavior of the dissipative sine-Gordon equation (1.2). The time average of $\sin \phi$ will be small, and, for sufficiently large p, the x derivatives can be neglected. Then (1.2) reduces to

$$\frac{dV}{dt} \approx -\alpha V . \qquad \text{(B-21)}$$

From (B-13), a breather forms every time V decreases by $2\pi/p$. Thus a rough estimate for the number of breathers formed per unit time and per unit distance is given by

$$\eta = \frac{\alpha V}{2\pi} . \qquad \text{(B-22)}$$

APPENDIX C: DOUBLE PHASE SOLUTIONS

This appendix is a summary account of the theory of multiphase solutions for nonlinear wave equations which has been developed over the past few years by Ablowitz [9 - 12].

Suppose we have a nonlinear wave equation for $\phi(x, t)$

$$N(\phi) = 0 \tag{C-1}$$

which can be obtained from an Euler variation of a Lagrangian density. Thus

$$N(\phi) = \frac{\delta}{\delta\phi} L(\phi_t, -\phi_x, \phi) . \tag{C-2}$$

Suppose further that $\phi(x, t)$ can be written as a double phase function

$$\phi(x, t) = \Phi(\theta_1, \theta_2) \tag{C-3}$$

such that L is a doubly periodic function of θ_1 and θ_2. Then choose

$$\theta_1 = \omega_1 t - k_1 x$$
$$\theta_2 = \omega_2 t - k_2 x \tag{C-4a,b}$$

and average L over both periods to

$$\mathcal{L} \equiv \frac{1}{4\pi^2} \int_0^{2\pi} \int_0^{2\pi} L(\omega_1\Phi_{\theta_1} + \omega_2\Phi_{\theta_2}, k_1\Phi_{\theta_1} + k_2\Phi_{\theta_2}, \Phi)\theta\theta_1 d\theta_2 \tag{C-5}$$
$$= \mathcal{L}(\omega_1, \omega_2, k_1, k_2) .$$

If ω_1, ω_2, k_1 and k_2 are not constant but allowed to vary slowly with x and t, two dynamic equations for this slow evolution can be obtained from Euler variations of $\mathcal{L}$ with θ_1 and θ_2. Thus

$$\frac{\delta}{\delta\theta_1}\mathcal{L} = 0 \Longrightarrow \left(\frac{\partial\mathcal{L}}{\partial\omega_1}\right)_t - \left(\frac{\partial\mathcal{L}}{\partial k_1}\right)_x = 0 \qquad \text{(C-6a)}$$

$$\frac{\delta}{\delta\theta_2}\mathcal{L} = 0 \Longrightarrow \left(\frac{\partial\mathcal{L}}{\partial\omega_2}\right)_t - \left(\frac{\partial\mathcal{L}}{\partial k_2}\right)_x = 0 . \qquad \text{(C-6b)}$$

Two additional equations are conservation of periods for the two components or

$$(\omega_1)_x + (k_1)_t = 0$$

$$(\omega_2)_x + (k_2)_t = 0 . \qquad \text{(C-6c,d)}$$

A necessary condition for this description to be valid is that the original equation (C-1) have the double phase solutions indicated in (C-3) for which L is doubly periodic. It has recently been demonstrated that multiple phase solutions [$\phi(x, t) = \Phi(\theta_1, \theta_2, \ldots, \theta_N)$ for any finite integer N] exist for those particular nonlinear wave equations which display soliton behavior [13-15]. This class includes the sine-Gordon equation (1.1).

A Lagrangian density for (1.1) is

$$L = \frac{1}{2}\phi_x^2 - \frac{1}{2}\phi_t^2 - \cos\phi . \qquad \text{(C-7)}$$

If $\phi(x, t)$ has the doubly periodic form in (C-3)

$$L = \frac{1}{2}(k_1\Phi_{\theta_1} + k_2\Phi_{\theta_2})^2 - \frac{1}{2}(\omega_1\Phi_{\theta_1} + \omega_2\Phi_{\theta_2})^2 - \cos\Phi \qquad \text{(C-8)}$$

so (C-6a,b) become

$$\frac{\partial}{\partial t}\int_0^{2\pi}\int_0^{2\pi}(\omega_1\Phi_{\theta_1}^2+\omega_2\Phi_{\theta_1}\Phi_{\theta_2})d\theta_1 d\theta_2 + \frac{\partial}{\partial x}\int_0^{2\pi}\int_0^{2\pi}(k_1\Phi_{\theta_1}^2+k_2\Phi_{\theta_1}\Phi_{\theta_2})d\theta_1 d\theta_2=0$$

$$\frac{\partial}{\partial t}\int_0^{2\pi}\int_0^{2\pi}(\omega_2\Phi_{\theta_2}^2+\omega_1\Phi_{\theta_1}\Phi_{\theta_2})d\theta_1 d\theta_2 + \frac{\partial}{\partial x}\int_0^{2\pi}\int_0^{2\pi}(k_2\Phi_{\theta_2}^2+k_1\Phi_{\theta_1}\Phi_{\theta_2})d\theta_1 d\theta_2 = 0. \qquad \text{(C-9a,b)}$$

These are (3.22) of reference [9].

Now consider (1.2) in which the sine-Gordon equation is made dissipative through addition of the small loss term $-\alpha\phi_t$. Following the discussion in Whitham [7, p. 510], we note that (C-9a) can be interpreted as

$$\langle\phi_t\rangle_{1t} - \langle\phi_x\rangle_{1x} + \langle\sin\phi\rangle_1 \equiv 0 \qquad \text{(C-10)}$$

where

$$\langle\cdot\rangle_1 \equiv \int_0^{2\pi}\int_0^{2\pi}(\cdot)\Phi_{\theta_1}d\theta_1 d\theta_2 . \qquad \text{(C-11)}$$

Noting the correspondence between (C-10) and (1.1) in the form

$\phi_{tt} - \phi_{xx} + \sin\phi = 0$, we can perform a similar averaging of (1.2) to obtain

$$\langle \phi_t \rangle_{1t} - \langle \phi_x \rangle_{1x} + \langle \sin\phi \rangle_1 = -\alpha \langle \phi_t \rangle_1 . \tag{C-12}$$

Similar treatment with respect to the averaging

$$\langle \cdot \rangle_2 \equiv \int_0^{2\pi} \int_0^{2\pi} (\cdot)\Phi_{\theta_2} d\theta_1 d\theta_2 \tag{C-13}$$

leads to the pair of dynamic equations

$$\frac{\partial}{\partial t}\int_0^{2\pi}\int_0^{2\pi} (\omega_1 \Phi_{\theta_1}^2 + \omega_2 \Phi_{\theta_1}\Phi_{\theta_2}) d\theta_1 d\theta_2 + \frac{\partial}{\partial x}\int_0^{2\pi}\int_0^{2\pi} (k_1 \Phi_{\theta_1}^2 + k\Phi_{\theta_1}\Phi_{\theta_2}) d\theta_1 d\theta_2 =$$

$$= -\alpha \int_0^{2\pi}\int_0^{2\pi} (\omega_1 \Phi_{\theta_1}^2 + \omega_2 \Phi_{\theta_1}\Phi_{\theta_2}) d\theta_1 d\theta_2$$

$$\frac{\partial}{\partial t}\int_0^{2\pi}\int_0^{2\pi} (\omega_2 \Phi_{\theta_2}^2 + \omega_1 \Phi_{\theta_1}\Phi_{\theta_2}) d\theta_1 d\theta_2 + \frac{\partial}{\partial x}\int_0^{2\pi}\int_0^{2\pi} (k_2 \Phi_{\theta_2}^2 + k_1 \Phi_{\theta_1}\Phi_{\theta_2}) d\theta_1 d\theta_2 =$$

$$= -\alpha \int_0^{2\pi}\int_0^{2\pi} (\omega_1 \Phi_{\theta_1}^2 + \omega_2 \Phi_{\theta_1}\Phi_{\theta_2}) d\theta_1 d\theta_2 .$$

(C-14a,b)

These, together with the conservation equations (C-6c,d) are the dynamic equations used in this paper. In Section III, only a single phase is assumed (3.3) so (C-14a) reduces to (3.5a). In Section IV, both phases are employed for the d.c. components. It is necessary in either case to assume

$\alpha \ll 1$

so that the dissipative variation over a cycle is small and the averaging indicated in (C-5) is well defined.

Ablowitz [9] has suggested a way to get some integral constraints on the function $\Phi(\theta_1, \theta_2)$. Considering (C-3) as a change of independent variables, (1.1) becomes

$$g_1\Phi_{\theta_1\theta_1} + 2h\Phi_{\theta_1\theta_2} + g_2\Phi_{\theta_2\theta_2} + \sin\Phi = 0 \qquad \text{(C-15)}$$

where $g_i \equiv \omega_i^2 - k_i^2$ and $h \equiv \omega_1\omega_2 - k_1k_2$. This equation can be written in the form of a conservation law as

$$\frac{\partial}{\partial\theta_1}\left(\frac{1}{\partial} g_1\Phi_{\theta_1}^2 - \frac{1}{2} g_2\Phi_{\theta_2}^2 - \cos\Phi\right) + \frac{\partial}{\partial\theta_2}\left(h\Phi_{\theta_1}^2 + g_2\Phi_{\theta_1}\Phi_{\theta_1}\right) = 0$$

or as (C-16a,b)

$$\frac{\partial}{\partial\theta_1}\left(h\Phi_{\theta_2}^2 + g_1\Phi_{\theta_1}\Phi_{\theta_2}\right) + \frac{\partial}{\partial\theta_2}\left(\frac{1}{2} g_2\Phi_{\theta_2}^2 - \frac{1}{2} g_1\Phi_{\theta_1}^2 - \cos\Phi\right) = 0.$$

From these it follows that

$$\int_0^{2\pi}\left(\frac{1}{2} g_1\Phi_{\theta_1}^2 - \frac{1}{2} g_2\Phi_{\theta_2}^2 - \cos\Phi\right)d\theta_2 = -E_1$$

and (C-17a,b)

$$\int_0^{2\pi}\left(\frac{1}{2} g_2\Phi_{\theta_2}^2 - \frac{1}{2} g_1\Phi_{\theta_1}^2 - \cos\Phi\right)d\theta_1 = -E_2 .$$

If Φ is independent of θ_2, (C-17a) is satisfied by the elliptic function in (3.4).

Under the assumption $h = 0$, (C-15) becomes

$$g_1 \Phi_{\theta_1 \theta_1} + g_2 \Phi_{\theta_2 \theta_2} + \sin \Phi = 0 \qquad \text{(C-18)}$$

which Lamb [36] has shown to have solutions of the form

$$\Phi = 4 \tan^{-1}[f(\theta_1) g(\theta_2)] \qquad \text{(C-19)}$$

where f and g are elliptic functions. This is the doubly periodic function suggested recently by Ben-Abraham [42]. For our purposes, however, the assumption $h = 0$ is too severe. It requires

$$\left(\frac{\omega_1}{k_1}\right)\left(\frac{\omega_2}{k_2}\right) = 1 \qquad \text{(C-20)}$$

which means that the two component traveling waves must have phase velocities in the same direction with one going faster than the characteristic velocity of (1.1) and the other slower.

From references [13-15] it seems that a simple prescription for constructing a more general double phase solution to (1.1) would be as follows: i) Express the elliptic function defined in (3.4) in terms of theta functions, ii) Augment the arguments of these theta functions from θ to $\theta_1 + \theta_2$, and iii) Check that the resulting expression is a solution of (1.1).

Acknowledgements

It is my pleasure to acknowledge helpful discussions with J. C. Berryman, D. J. Kaup and D. W. McLaughlin.

REFERENCES

1. A. C. Scott and W. J. Johnson, Internal flux motion in large Josephson junctions, Appl. Phys. Lett. 14 (1969), 316-318.

2. A. Barone, Flux-flow effect in Josephson tunnel junctions, J. Appl. Phys. 42 (1971), 2747-2751.

3. A. Barone, Thermal effect in U-I characteristic of large Josephson junctions, Phys. Status Solidi 13 (1972), K93-K95.

4. M. J. Ablowitz, D. J. Kaup, A. C. Newell and H. Segur, Method for solving the sine-Gordon equation, Phys. Rev. Lett. 30 (1973), 1262-1264.

5. M. J. Ablowitz, D. J. Kaup, A. C. Newell and H. Segur, The inverse scattering transform-Fourier analysis for nonlinear problems, Studies in Appl. Math. 53 (1974), 249-315.

6. D. J. Kaup, Method for solving the sine-Gordon equation in laboratory coordinates, Studies in Appl. Math. 54 (1975), 165-179.

7. G. B. Whitham, Linear and nonlinear waves, Wiley-Interscience, New York (1974).

8. E. N. Pelinovskii and S. X. Shavratzkii On the damping of stationary waves in a system described by a nonlinear Klein-Gordon equation, Zhurnal Prikladnoi Mekhaniki i Tekkincheskoi Fisiki 5 (1974), 55-59, (in Russian; translation available from The Librarian, Math. Res. Center, University of Wisconsin, Madison).

9. M. J. Ablowitz and D. J. Benney, The evolution of multi-phase modes for nonlinear dispersive waves, Studies in Appl. Math. 49 (1970), 225-238.

10. M. J. Ablowitz, Applications of slowly varying nonlinear dispersive wave theories, Studies in Appl. Math. 50 (1971), 329-344.

11. M. J. Ablowitz, Approximate methods for obtaining multiphase modes in nonlinear dispersive wave problems, Studies in Appl. Math. 51 (1972), 17-55.

12. M. J. Ablowitz, A note on resonance and nonlinear dispersive waves, Studies in Appl. Math. 54 (1975), 61-70.

13. B. A. Dubrovin and S. P. Novikov, Periodic and conditionally periodic analogs of the many-soliton solutions of the Kortweg-de Vries equation, Sov. Phys. JETP, 40 (1975), 1058-1063.

14. A. R. Its and V. B. Mateev , Schrödinger operators with finite-gap spectrum and N-soliton solutions of the Korteweg-de Vries equation, Teoreticheskaya i Matematicheskaya Fisika, 23 (1975), 51-68. Translated by Plenum Publishing Corporation (1976).

15. E. Date and S. Tanaka, Analogue of inverse scattering theory for discrete Hill's equation and exact solutions for the periodic Toda lattice (preprint, 1976).

16. A. C. Scott, Propagation of magnetic flux on a long Josephson tunnel junction, Il Nuovo Cimento 69B (1970), 241-261.

17. A. C. Scott, F. Y. F. Chu and S. A. Reible, Magnetic flux propagation on a Josephson transmission line, J. Appl. Phys. (in press).

18. J. R. Waldram, A. B. Pippard and J. Clarke, Theory of the current-voltage characteristics of SNS junctions and other superconducting weak links, Philos. Trans. Roy. Soc. London 268 (1970), 265-287.

19. T. A. Fulton and R. C. Dynes, Single vortex propagation in Josephson tunnel junctions, Solid State Communications 12 (1973), 57-61.

20. T. A. Fulton, R. C. Dynes and P. W. Anderson, The flux shuttle-a Josephson junction shift register employing single flux quanta, Proc. IEEE 61 (1973), 28-35.

21. T. A. Fulton and L. N. Dunkleberger, Experimental flux shuttle, Appl. Phys. Lett. 22 (1973), 232-233.

22. K. Nakajima, T. Yamashita and Y. Onodera, Mechanical analog of active Josephson transmission line, J. Appl. Phys. 45 (1974), 3141-3145.

23. K. Nakajima, Y. Onodera, T. Nakamura and R. Sato, Numerical analysis of vortex motion on Josephson structures, J. Appl. Phys. 45 (1974), 4095-4099.

24. K. Nakajima, Y. Sawada and Y. Onodera, Nonequilibrium stationary coupling of solitons, J. Appl. Phys. 46 (1975), 5272-5279.

25. K. Nakajima, Y. Onodera and Y. Ogawa, Logic design of Josephson network, J. Appl. Phys. 47 (1976), 1620-1627.

26. A. C. Scott, Active and nonlinear wave propagation in electronics, Wiley-Interscience, New York (1970).

27. I. Giaever, Metal-insulator-metal tunneling phenomena in solids, Plenum Press, New York (1969), 19-30.

28. B. D. Josephson, Supercurrents through barriers, Advances in Phys. 14 (1965), 419-451.

29. W. J. Johnson and A. Barone, Effect of junction geometry on maximum zero-voltage Josephson current, J. Appl. Phys 41 (1970), 2958-2960. JAP 41 (1970), 2958.

30. M. D. Fiske, Temperature and magnetic field dependencies of the Josephson tunneling current, Rev. Mod. Phys. 36 (1964), 221-222.

31. I. M. Dmitrenko, I. K. Yanson and V. M. Svistunov, Interaction of the alternating Josephson current with resonant modes in a superconducting tunnel structure, JETP Lett. 2 (1965), 10-13.

32. I. O. Kulik, Theory of "steps" of voltage-current characteristic of the Josephson tunnel current, JETP Lett. 2 (1965), 84-87.

33. D. N. Langenberg, D. J. Scalapino and B. N. Taylor, Josephson-type superconducting tunnel junctions as generators of microwave and submillimeter wave radiation, Proc. IEEE 54 (1966), 560-575.

34. A. Barone, G. Paternò, M. Russo and R. Vaglio, Light-induced transition from "small" to "large" Josephson junctions, Phys. Lett. 53A (1975), 393-394.

35. D. W. McLaughlin and A. C. Scott, A restricted Bäcklund transformation, J. Math. Phys. 14 (1973), 1817-1828.

36. G. L. Lamb, Jr., Analytical descriptions of ultrashort optical pulse propagation in a resonant medium, Rev. Mod. Phys. 43 (1971), 99-124.

37. L. D. Faddeev, Hadrons from leptons ? JETP Lett. 21 (1975), 64-65.

38. V. E. Korepin, P. P. Kulish, and L. D. Faddeev, Soliton quantization, JETP Lett. 21 (1975), 138-139.

39. R. F. Dashen, B. Hasslacher and A. Neveu, Particle spectrum in model field theories from semiclassical functional integral techniques, Phys. Rev. D 11 (1975), 3424-3450.

40. A. C. Scott, Quantum theory of the small Josephson junction, Phys. Lett. 25A (1967), 132-133.

41. F. Y. F. Chu and A. C. Scott, Bäcklund transformations and the inverse method, Phys. Lett. 47A (1974), 303-304.

42. S. I. Ben-Abraham, Exact solution to the sine-Gordon equation in two space dimensions, Phys. Lett. 55A (1976), 383-384.

UNCLASSIFIED

SECURITY CLASSIFICATION OF THIS PAGE (When Data Entered)

REPORT DOCUMENTATION PAGE	READ INSTRUCTIONS BEFORE COMPLETING FORM
1. REPORT NUMBER: 1649 ✓	2. GOVT ACCESSION NO.
3. RECIPIENT'S CATALOG NUMBER	
4. TITLE (and Subtitle): MAGNETIC FLUX ANNIHILATION IN A LARGE JOSEPHSON JUNCTION ✓	5. TYPE OF REPORT & PERIOD COVERED: Summary Report - no specific reporting period
	6. PERFORMING ORG. REPORT NUMBER
7. AUTHOR(s): Alwyn C. Scott	8. CONTRACT OR GRANT NUMBER(s): DAAG29-75-C-0024 ✓ ENG 75-08492
9. PERFORMING ORGANIZATION NAME AND ADDRESS: Mathematics Research Center, University of Wisconsin ✓ 610 Walnut Street Madison, Wisconsin 53706	10. PROGRAM ELEMENT, PROJECT, TASK AREA & WORK UNIT NUMBERS
11. CONTROLLING OFFICE NAME AND ADDRESS: See item 18 below.	12. REPORT DATE: July 1976
	13. NUMBER OF PAGES: 62
14. MONITORING AGENCY NAME & ADDRESS (if different from Controlling Office)	15. SECURITY CLASS. (of this report): UNCLASSIFIED
	15a. DECLASSIFICATION/DOWNGRADING SCHEDULE

16. DISTRIBUTION STATEMENT (of this Report)

Approved for public release; distribution unlimited.

17. DISTRIBUTION STATEMENT (of the abstract entered in Block 20, if different from Report)

18. SUPPLEMENTARY NOTES

U.S. Army Research Office
P.O. Box 12211
Research Triangle Park
North Carolina 27709

National Science Foundation
Washington, D. C. 20550

19. KEY WORDS (Continue on reverse side if necessary and identify by block number)

Sine-Gordon equation
Kink
Breather
Whitham's method
Inverse scattering transform method
Fluxon annihilation

20. ABSTRACT (Continue on reverse side if necessary and identify by block number)

Recent developments in the theory of the sine-Gordon equation are used to analyze the appearance of a 'displaced linear branch' in the volt-ampere characteristic of a large Josephson junction. Internally the junction

→ next page (continued)

DD FORM 1 JAN 73 1473 EDITION OF 1 NOV 65 IS OBSOLETE

UNCLASSIFIED

SECURITY CLASSIFICATION OF THIS PAGE (When Data Entered)

cont. → is divided into a flux annihilation domain near the center and flux flow domains near the edges. The displaced linear branch is experimental evidence for the existence of flux flow domains. In the flux annihilation domain, an ac voltage component is induced by the continuous formation and decay of sine-Gordon breathers. Whitham's nonlinear WKB method is used to analyze the flux flow domains while the inverse scattering transform method is used as a qualitative guide to the study of breather formation in the flux annihilation domain.